

6-2019

Estuarine Dissolved Organic Carbon Flux From Space: With Application to Chesapeake and Delaware Bays

Sergio R. Signorini

Antonio Mannino

Marjorie A.M. Friedrichs

Pierre St-Laurent

John Wilkin

See next page for additional authors

Follow this and additional works at: https://digitalcommons.odu.edu/ccpo_pubs



Part of the [Climate Commons](#), [Fresh Water Studies Commons](#), and the [Oceanography Commons](#)

Original Publication Citation

Signorini, S. R., Mannino, A., Friedrichs, M. A. M., Pierre, S. L., Wilkin, J., Tabatabai, A., . . . Yao, Y. (2019). Estuarine dissolved organic carbon flux from space: With application to Chesapeake and Delaware Bays. *Journal of Geophysical Research: Oceans*, 124(6), 3755-3778. doi:10.1029/2018JC014646

This Article is brought to you for free and open access by the Center for Coastal Physical Oceanography at ODU Digital Commons. It has been accepted for inclusion in CCPO Publications by an authorized administrator of ODU Digital Commons. For more information, please contact digitalcommons@odu.edu.

Authors

Sergio R. Signorini, Antonio Mannino, Marjorie A.M. Friedrichs, Pierre St-Laurent, John Wilkin, Aboozar Tabatabai, Raymond G. Najjar, Eileen E. Hofmann, Fei Da, Hanqin Tian, and Yuanzhi Yao

RESEARCH ARTICLE

10.1029/2018JC014646

Special Section:

Carbon cycling in tidal wetlands and estuaries of the contiguous United States

Key Points:

- Temporal variability of DOC export out of the Chesapeake and Delaware Bays is largely driven by freshwater discharge into the bays
- Differences in DOC export between the two bays are driven primarily by their geomorphology and freshwater inputs
- Terrestrial DOC inputs are similar to bay mouth DOC export at annual and longer time scales but diverge at time scales of days to months

Supporting Information:

- Supporting Information S1
- Figure S1
- Figure S2

Correspondence to:

S. R. Signorini,
sergio.signorini@nasa.gov

Citation:

Signorini, S. R., Mannino, A., Friedrichs, M. A. M., St-Laurent, P., Wilkin, J., Tabatabai, A., et al (2019). Estuarine dissolved organic carbon flux from space: With application to Chesapeake and Delaware Bays. *Journal of Geophysical Research: Oceans*, 124, 3755–3778. <https://doi.org/10.1029/2018JC014646>












Received 7 OCT 2018

Accepted 15 APR 2019

Accepted article online 23 APR 2019

Published online 13 JUN 2019

Estuarine Dissolved Organic Carbon Flux From Space: With Application to Chesapeake and Delaware Bays

Sergio R. Signorini¹ , Antonio Mannino² , Marjorie A. M. Friedrichs³ , Pierre St-Laurent³ , John Wilkin⁴ , Aboozar Tabatabai⁴ , Raymond G. Najjar⁵ , Eileen E. Hofmann⁶ , Fei Da³ , Hanqin Tian⁷ , and Yuanzhi Yao⁷ 

¹NASA Goddard Space Flight Center and Science Applications International Corporation, Greenbelt, MD, USA, ²NASA Goddard Space Flight Center, Greenbelt, MD, USA, ³Virginia Institute of Marine Science, William & Mary, Gloucester Point, VA, ⁴Department of Marine and Coastal Sciences, Rutgers, The State University of New Jersey, New Brunswick, NJ, USA, ⁵Department of Meteorology and Atmospheric Science, The Pennsylvania State University, University Park, PA, USA, ⁶Center for Coastal Physical Oceanography, Department of Ocean, Earth and Atmospheric Sciences, Old Dominion University, Norfolk, VA, USA, ⁷International Center for Climate and Global Change Research and School of Forestry and Wildlife Sciences, Auburn University, Auburn, AL, USA

Abstract This study uses a neural network model trained with in situ data, combined with satellite data and hydrodynamic model products, to compute the daily estuarine export of dissolved organic carbon (DOC) at the mouths of Chesapeake Bay (CB) and Delaware Bay (DB) from 2007 to 2011. Both bays show large flux variability with highest fluxes in spring and lowest in fall as well as interannual flux variability (0.18 and 0.27 Tg C/year in 2008 and 2010 for CB; 0.04 and 0.09 Tg C/year in 2008 and 2011 for DB). Based on previous estimates of total organic carbon (TOCexp) exported by all Mid-Atlantic Bight estuaries (1.2 Tg C/year), the DOC export (CB + DB) of 0.3 Tg C/year estimated here corresponds to 25% of the TOCexp. Spatial and temporal covariations of velocity and DOC concentration provide contributions to the flux, with larger spatial influence. Differences in the discharge of fresh water into the bays (74 billion m³/year for CB and 21 billion m³/year for DB) and their geomorphologies are major drivers of the differences in DOC fluxes for these two systems. Terrestrial DOC inputs are similar to the export of DOC at the bay mouths at annual and longer time scales but diverge significantly at shorter time scales (days to months). Future efforts will expand to the Mid-Atlantic Bight and Gulf of Maine, and its major rivers and estuaries, in combination with coupled terrestrial-estuarine-ocean biogeochemical models that include effects of climate change, such as warming and CO₂ increase.

Plain Language Summary This study combines satellite data, field work observations, and statistical and numerical models to investigate the seasonal and interannual variability of dissolved organic carbon (DOC) export from two major East Coast estuaries, Chesapeake, and Delaware Bays. DOC is a food supplement, supporting growth of microorganisms and plays an important role in the global carbon cycle through the microbial loop, a marine pathway which incorporates DOC into the food chain. Using this novel methodology, we were able to better quantify the combined contribution of these estuaries to the East Coast carbon budget and contrast estuarine properties affecting the DOC export, such as riverine inputs, time scales of variability, and geomorphology. The combined DOC contribution of these two estuaries represents 25% of the total organic carbon exported by all Mid-Atlantic Bight (the coastal region running from Massachusetts to North Carolina) estuaries, and 27% of the total atmospheric carbon dioxide uptake in the Mid-Atlantic Bight.

1. Introduction

An important flux in the global carbon cycle is the transfer of carbon from land to ocean via rivers, groundwater, and tidal exchange with wetlands. The riverine dissolved organic carbon (DOC) portion of this flux is highly variable (Fransner et al., 2016; Meng et al., 2017; Wu et al., 2017) and on a global scale is able to sustain the inventory of DOC in the ocean (Bauer & Bianchi, 2011), a reservoir of carbon that is of approximately the same size as the atmospheric CO₂ reservoir (Ciais et al., 2013). However, the quantity and quality of riverine carbon delivered to the ocean depends on estuarine processes, such as photosynthesis, respiration, photochemical oxidation, burial, and gas exchange. For example, on a global basis, estuaries are believed to outgas roughly 20% of the carbon delivered to them from rivers and tidal wetlands (Bauer et al.,

2013). A recent study of the estuaries along the east coast of North America estimated that these estuaries outgas ~38% of the total carbon entering from rivers and tidal wetlands and laterally export ~57% of this carbon to the ocean (Najjar et al., 2018).

Of the various fluxes that make up estuarine carbon budgets, one of the most uncertain is the exchange between the estuary and the ocean. In theory, this flux can be directly determined if simultaneous and continuous measurements of carbon concentration and velocity across the mouth of an estuary are available. However, such a direct determination of estuary-ocean carbon exchange is generally not practical for large estuaries, as tidal currents typically require continuous measurements of carbon concentrations through space (depth and cross-channel) and time at very high resolution.

Studies have estimated this estuary-ocean exchange indirectly with methods that employ concentration-salinity relationships, box models, mass balance, or three-dimensional mechanistic models. Methods employing concentration-salinity relationships and box models both require measurements of carbon concentration, salinity, and streamflow. The concentration-salinity relationship method, which has been used to estimate the export of organic (Raymond & Bauer, 2001) and inorganic carbon (Amann et al., 2015; Cai et al., 2000; Cai & Wang, 1998; Gazeau et al., 2005; Maher & Eyre, 2012; Raymond et al., 2000) from estuaries to the ocean has the advantage of simplicity but is limited by the assumption of a 1-D (along the axis of the estuary) steady state (Boyle et al., 1974; Kaul & Froelich, 1984; Liss, 1976; Officer, 1979). Hence, some spatial (e.g., vertical stratification) and temporal (e.g., tides) complexities that may significantly alter carbon fluxes are ignored. The box model method estimates carbon flux using exchange coefficients derived from salt and water balances (Crosswell et al., 2017; Ford et al., 2005; McGuirk Flynn, 2008; Samanta et al., 2015; Wang & Cai, 2004) and has the advantage of being flexible enough to relax assumptions of 1-D and steady state, but is again limited in time and space resolution by the availability of observations. The combined measurements of carbon concentrations at three depths near the mouth of an estuary with velocity from a one-dimensional (1-D) hydrodynamic model, appears to be the closest any study has come to a direct determination of estuary-ocean carbon exchange (Winter et al., 1996). In the mass balance method for computing estuary-ocean exchange, all other terms of the estuarine carbon budget are estimated and the exchange is computed as a residual, assuming steady state mass balance (Crosswell et al., 2017; Herrmann et al., 2015; Najjar et al., 2018). In addition to the steady state assumption, this method is limited by the accuracy of the other budget terms, which themselves may be determined indirectly and have large errors.

Linked hydrodynamic-biogeochemical mechanistic models used to estimate estuary-ocean exchange include explicit representation of the key processes that affect carbon in estuaries, such as advection, gas exchange, photosynthesis, and respiration. These models range in hydrodynamic complexity from 1-D, tidally averaged, advection-diffusion models (Hofmann et al., 2008; Laruelle et al., 2017; Soetaert & Herman, 1995; Volta et al., 2016) to 3-D tidally resolving models (Cercó & Cole, 1993; Feng et al., 2015; Kemp et al., 1997). Biogeochemical complexity can be measured by the number of state variables, which ranges from six (Vanderborcht et al., 2007) to 20 (Cercó & Cole, 1993; Soetaert & Herman, 1995). Advantages of mechanistic models include the relaxation of the steady state assumption and the potential to resolve a multitude of time scales, from tidal to interannual. However, mechanistic models require extensive data sets for model evaluation and can be difficult to calibrate due to numerous poorly constrained parameters.

Collectively, the above studies on estuary-ocean exchange of carbon demonstrate the importance of this exchange in estuarine carbon budgets and its dependence on estuarine net ecosystem production, CO₂ exchange with the atmosphere, and burial. Estuary-ocean exchange of carbon and related quantities (e.g., nutrients, oxygen, and alkalinity) is thus not only important for understanding the land-ocean link in global biogeochemical cycles but is an important metric of biogeochemical processing within an estuary.

With estuarine biogeochemical and physical processes responding to forcing at a variety of time scales, including tidal, weather-related, seasonal, and climatic (both natural and anthropogenic), it is likely that estuary-ocean carbon exchange also has high variability. Indeed, there is evidence for variability in estuary-ocean carbon exchange at tidal (Winter et al., 1996), seasonal (Wang & Cai, 2004), and interannual (Crosswell et al., 2017) time scales. Spatial variability of the exchange along an estuary mouth may be considerable as well because of complex estuarine hydrodynamics that lead to vertical and horizontal separation of landward and seaward flows (Valle-Levinson et al., 1998). Capturing with in situ observations, the multiple scales of this temporal and spatial variability in estuary-ocean exchange is demanding and

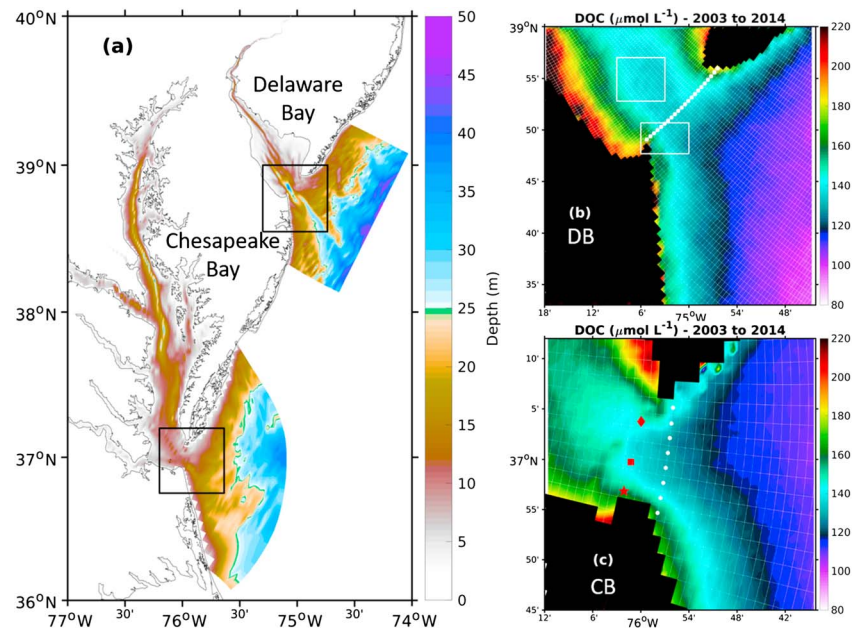


Figure 1. Model bathymetry for the CB and DB models (a). Twelve-year (2003–2014) mean MODIS DOC for DB (b) and CB (c) with ROMS grid lines superposed in white and land mask in black. The white dots across the bay mouths are the grid points used in the flux computation. The squares in (a) correspond to the size (50 km \times 50 km) and location of the DB and CB MODIS images shown in (b) and (c). The boxes near DB mouth in (b) delimit the cluster of available in situ data stations. The red star, red square, and red diamond near CB mouth in (c) are the locations of CBP in situ data stations CB8.1E, CB7.4, and CB7.4 N, respectively. CB = Chesapeake Bay; DB = Delaware Bay; MODIS = Moderate Resolution Imaging Spectroradiometer.

requires novel approaches beyond the usual monthly sampling of many coastal water quality monitoring programs.

Remote sensing has the potential to alleviate some of the challenges associated with estimating estuary-ocean exchange (Mannino et al., 2016). Satellite retrievals of dissolved and particulate organic carbon have been made in numerous coastal regions (Brezonik et al., 2015; Del Castillo & Miller, 2008; Fichot et al., 2014; Fichot & Benner, 2011; Hoge et al., 1995; Mannino et al., 2008, 2014, 2016; Matsuoka et al., 2017; Slonecker et al., 2016; Son et al., 2009). In order to determine carbon transport, simultaneous estimates of the velocity field are needed as well. Mannino et al. (2016) developed an approach to quantify DOC transport in a coastal shelf region by combining remote sensing retrievals of DOC with hydrodynamic model estimates of velocity (see also Cui et al., 2018). Here, this approach is adopted to quantify estuary-ocean DOC exchange for two coastal-plain estuaries, Chesapeake Bay (CB) and Delaware Bay (DB). This view of estuary-ocean DOC exchange is unprecedented in that it combines multiple sources of data and captures vertical, horizontal, and temporal (daily resolution over 5 years) variability in the exchange. To help interpret the large temporal variability observed, the results are compared with riverine inputs computed from a terrestrial biogeochemical model.

2. Study Regions

Chesapeake and Delaware Bays are large, coastal plain estuaries located in the northeast United States (Figure 1a). Table 1 summarizes some of the most relevant physical and biogeochemical properties of the two bays. Surface area, volume, and watershed area are all much larger for CB than for DB. Given that the watersheds of CB and DB experience relatively similar climates and assortment of land uses, watershed area is the main factor that explains the differences in riverine input of freshwater, carbon, and nitrogen to the two estuaries.

Like many temperate estuaries, freshwater flow to CB and DB has strong seasonal and interannual variability. The ratio of 1998–2014 mean flow in March (month of maximum flow) to mean flow in August (month

Table 1
Summary of Physical and Biogeochemical Properties of Chesapeake and Delaware Bays (CB and DB)

Property	Chesapeake bay	Delaware bay	DB/CB
Surface area (km ²)	11,500 ^a	2,030 ^b	0.18
Estuary volume ^c (km ³)	77	19	0.25
Residence time (days)	180 ^d	68 ^e	0.38
Watershed area ^f (km ²)	160,765	30,792	0.19
Average river discharge ^g (m ³ /s)	2345	667	0.28
Riverine DOC input ^g (Tg C/year)	0.216	0.058	0.27
Riverine POC input ^g (Tg C/year)	0.092	0.026	0.28
Riverine nitrogen input ^h (Tg N/year) ^f	0.152	0.053	0.35
Riverine DOC yield ^g (Tg C·km ⁻² ·year ⁻¹)	1.34×10^{-6}	1.88×10^{-6}	1.4
Riverine POC yield ^g (Tg C·km ⁻² ·year ⁻¹)	0.572×10^{-6}	0.844×10^{-6}	1.48
Riverine nitrogen yield ^h (Tg N·km ⁻² ·year ⁻¹) ^f	0.945×10^{-6}	1.72×10^{-6}	1.82
Mean primary prod. (Tg C/year) ⁱ	4.43 ^j	0.62 ^c	0.14
Area-specific primary prod. (Tg C·km ⁻² ·year ⁻¹)	3.85×10^{-4}	3.05×10^{-4}	0.79

Note. Ratios (DB/CB) for all properties are included for comparison.

^aKemp et al. (2005); ^bhttps://en.wikipedia.org/wiki/Delaware_Bay; ^cPennock and Sharp (1986); ^dDu and Shen (2016); ^eM. Herrmann (personal communication, October 2017); ^fCastro et al. (2001); ^gDLEM (1979–2015; see section 3.5); ^hStanley, 2001; based on Nixon et al., 1996; includes atmospheric deposition, land drainage, and sewage for DB; ⁱConverted to area integrated production from original source in g·m⁻²·year⁻¹. Yield refers to normalization of riverine input to watershed area; ^jHarding et al. (2002)

of minimum flow) is 2.3 for DB and 3.1 for CB. Interannual variability in freshwater flow to these estuaries is about a factor of 2 larger than interannual variability in precipitation on a fractional basis (Najjar et al., 2009). The two estuaries are also similar in that the freshwater input is dominated by a single river emptying into the main stem of the estuary (~50% from the Susquehanna River for CB and ~58% from the Delaware River for DB, (Schubel & Pritchard, 1986; Smullen et al., 1983). Each estuary also has significant freshwater input from a range of large and small rivers. Despite these similarities in freshwater forcing, the patterns of circulation and stratification in the two estuaries differ considerably. Tidal amplitude is greater in DB, in part due to differences in shape of the two bays, funnel for DB and dendritic for CB (Ross et al., 2017). Stronger tides in DB and a deeper central channel in CB (Figure 1a) lead to DB being relatively well mixed (Sharp et al., 1986) and CB being partially stratified (Schubel & Pritchard, 1986). While the two estuaries are similar in width at the mouths, the deep channel on the south side of the DB mouth yields a much larger cross-sectional area than in CB (Figure 1a).

Freshwater input and circulation are key drivers of biogeochemical processes in DB and CB. Circulation in CB is characterized by a lower-layer landward flow that acts to retain particulate and dissolved materials in the bay (Pritchard, 1956, 1967), leading to a relatively long residence time (180 days, Table 1) for freshwater and nutrients (Du & Shen, 2016). The combination of the bay's long water residence time, its stratified water column, and its narrow central channel isolated by sills and flanked by wide shallows make this a productive system, with efficient nutrient use and tendency for depletion of oxygen within deep waters (Boicourt, 1992). Use of nutrients in DB appears to be less efficient, as indicated by a relatively high DB/CB ratio of riverine nitrogen yield and correspondingly low DB/CB ratio for area-specific primary production (Table 1). The riverine yields (in Tg·km⁻²·year⁻¹) were defined as the riverine loads (in Tg/year) divided by the watershed area (in km²). The relatively low productivity of DB may reflect the short residence time of this estuary as well as the strong light limitation of phytoplankton growth (Pennock & Sharp, 1986).

Numerous studies underscore the wide range of processes that contribute to spatial and temporal variability of DOC in CB and DB. Satellite products for CB and DB highlight strong horizontal gradients in surface DOC and temporal variability that reflects processes due to tides, extreme riverine discharge events, seasonal changes in biogeochemistry and circulation, and climate variability (Cao et al., 2018). As in most estuaries, DOC concentrations in CB and DB generally decrease with salinity, indicating the important input of high-DOC waters from rivers (Fisher et al., 1998; Raymond & Bauer, 2001; Rochelle-Newall & Fisher, 2002; Sharp et al., 2009). DOC production in CB occurs under high-chlorophyll and high-turbidity conditions (Fisher et al., 1998), suggesting sources from primary production and solubilization of particulate organic carbon (POC). Higher DOC release by phytoplankton likely occurs under nutrient-stressed conditions (Anderson

& Williams, 1998; Druon et al., 2010; Fisher et al., 1998; Mannino et al., 2008, 2016), which occur during the summer, when stratification and light availability are high. There is a very large body of literature addressing the ability of phytoplankton to secrete DOC in the form of TEP (transparent exopolymeric material). An informative review is provided in Decho and Gutierrez (2017). Other important sources to these estuaries are lateral inputs from tidal wetlands (Axelrad et al., 1976; Jordan et al., 1983; Jordan & Correll, 1991; Roman & Dalber, 1989) and bottom sediments (Burdige & Homstead, 1994). Molecular characterization of DOC in CB and DB also supports in situ production as well as profound transformations of DOC of terrestrial origin (Harvey & Mannino, 2001; Mannino & Harvey, 1999, 2000a, 2000b; Mitra et al., 2000). While detailed studies are lacking for CB and DB (Bauer & Bianchi, 2011), the available evidence suggests that microbial consumption of DOC is a dominant loss process of DOC in terms of carbon remineralization, but photochemical degradation of DOC is relatively minor (Russ & Mannino, 2006, personal communication). In summary, these two large estuaries are effective biogeochemical reactors for many of their organic and inorganic constituents and therefore play a major role in regulating the flux of DOC between their adjacent terrestrial and continental shelf ecosystems.

3. Methods

3.1. NnetM Strategy

The neural networks model (NnetM) was designed to enable the computation of the integrated DOC tracer flux from satellite retrievals of DOC concentrations and numerical model products. The methodology is described in Mannino et al. (2016), and thus, only a brief description is provided here. A feed-forward neural networks scheme (Beale et al., 2018) is trained with observations and applied to produce normalized vertical DOC profiles using location, temperature (T), and salinity (S) as inputs to the NnetM. About 80% of the data is used to train the model and the other 20% to determine its statistical performance. Successive passes are performed on the data set until the best fit is achieved.

The DOC concentrations at each model grid location (i, j), time (t), and depth level (k) are obtained from the product of the NnetM profiles (normalized by the maximum value of each profile ($\text{DOC}_{\text{NnetM}}^{\text{max}}$) and the satellite DOC (DOC_{Sat}),

$$\text{DOC}(i, j, k, t) = \text{DOC}_{\text{Sat}}(i, j, t) \times \text{DOC}_{\text{NnetM}}(i, j, k, t) / \text{DOC}_{\text{NnetM}}^{\text{max}}(i, j, k, t) \quad (1)$$

The integrated DOC tracer flux component normal to the transect across the estuary mouth (F_{nu} for CB and F_{nv} for DB) is then computed at each grid point (Figures 1b and 1c) as

$$F_{\text{nu}}(t) = \sum_{i=1}^n \sum_{k=-h}^{k=0} [\text{DOC}(i, j_{\text{cte}}, k, t) u(i, j_{\text{cte}}, k, t) \Delta z \Delta x] \quad (2)$$

$$F_{\text{nv}}(t) = \sum_{j=1}^n \sum_{k=-h}^{k=0} [\text{DOC}(i_{\text{cte}}, j, k, t) v(i_{\text{cte}}, j, k, t) \Delta z \Delta y] \quad (3)$$

Following the Regional Ocean Modeling System (ROMS) grid orientation for each bay, equation (2) was used for CB (u component perpendicular to the cross section) and equation (3) for DB (v component perpendicular to the cross section). Thus, index j was kept at a constant value (cte) in (2) and index i kept constant in (3). The fluxes were integrated at daily averaged intervals from the bottom (h) to the surface, and along the n grid points of the cross sections. The areas of each cross-section grid cell are shown as the product of depth (Δz) and width ($\Delta x, \Delta y$) of each cell ($\Delta z \Delta x$ and $\Delta z \Delta y$). The grid cell water volume fluxes for CB ($u \Delta z \Delta x$) and DB ($v \Delta z \Delta y$) were computed and stored during the numerical model runs.

In situ profiles of DOC, T , and S to train and evaluate the NnetM were obtained from available field data (Mannino et al., 2014) and literature (Bauer et al., 2001, 2002; Guo et al., 1995). The data described in Mannino et al. (2014) were collected on multiple cruises from May 2004 to February 2013 within the Mid-Atlantic Bight (MAB, the coastal region running from Massachusetts to North Carolina) and estuaries of the MAB including Chesapeake Bay, Delaware Bay, and the Hudson-Raritan Estuary (system of bays and tidal rivers where the Hudson, Hackensack, Passaic, Rahway, and Raritan Rivers meet the Atlantic Ocean). The NnetM used here was trained with the same data set used in our previous study of the MAB (Mannino et al., 2016).

The DOC vertical profiles were derived using the neural network model trained and tested with 1,180 observations of temperature (2.4 to 29 °C), salinity (0.5 to 36.2 p.s.u.), DOC (40.6 to 242.1 mmol/m³) from depths ranging from the surface to a maximum of 500 m (shelf break). The neural network architecture was designed to minimize overfitting of the data to allow for predictions outside the range of values used to train the model, which should include deviations caused by climate change as long as the physical model is capable of providing accurate temperature and salinity predictions. The climate change impact on rates of remineralization and production of DOC are not directly predicted by the neural network model. Another limitation is the length of the available satellite ocean color time series, currently 1998–present (nearly 22 years) if SeaWiFS and MODIS Aqua sensors are combined, which falls short of a multidecadal climate record for the required algorithm retrievals.

3.2. Numerical Models

The estuarine model products (T , S , u , v) were obtained from the Chesapeake Bay Estuarine Carbon Biogeochemistry model (Da et al., 2018; Feng et al., 2015; Irby & Friedrichs, 2019) and a similar Delaware Bay model implementation (Tabatabai, 2017) for the concurrent period of analysis (2007–2011). Both models are based on the open-source community ROMS. For computational efficiency and accuracy, the volume transport (in m³/s) components at each grid cell and each time step were calculated internally in the ROMS implementation, $u\Delta z\Delta y$ and $v\Delta z\Delta x$, and archived for later use to compute the DOC integrated tracer flux. ChesROMS-ECB was forced with river inputs from a mechanistic terrestrial biogeochemical model (the Dynamic Land Ecosystem Model, DLEM; Tian et al., 2015; Yang, Tian, Friedrichs, Hopkinson, et al., 2015; Yang, Tian, Friedrichs, Liu, et al., 2015), whereas the Delaware model was forced with freshwater inputs from United States Geological Survey gauge information.

For the Delaware Bay model tidal flow and elevation were extracted from a simulation by the Advanced Circulation Model for Oceanic, Coastal, and Estuarine Waters (Mukai et al., 2002) with seven harmonic constituents; K1, O1, Q1, M2, S2, N2, and K2 at the boundaries. Bulk formulas (Fairall et al., 2003) were used in the model to calculate momentum and heat transfer at air-sea interface. The required information, including wind, temperature, humidity, pressure, downward solar short-wave radiation, and reflecting long-wave radiation, was compiled from NOAA's North American Regional Reanalysis (NARR, Mesinger et al., 2006). Similarly, all atmospheric forcing fields for the Chesapeake Bay ROMS are from the NARR (Mesinger et al., 2006), and the tidal forcing is from Advanced Circulation Model for Oceanic, Coastal, and Estuarine Waters (Luettich & Westerink, 1991; Mukai et al., 2002).

The along-transect average grid resolution is 1.88 km for CB (Figure 1b) and 0.60 km for DB (Figure 1c). Only products originating from the physical components of the models were used in this study.

3.3. Satellite DOC Algorithm

The retrieval of the satellite DOC is a two-step process. First, an algorithm (Mannino et al., 2014) is applied to retrieve absorption of chromophoric dissolved organic matter at 412 nm (aCDOM₄₁₂). This requires the input of reflectances at 443 and 547 nm when using the algorithm derived for the Moderate Resolution Imaging Spectroradiometer (MODIS) Aqua bands. The second step is to retrieve the DOC concentration derived as a function of aCDOM₄₁₂ using the algorithm of Mannino et al. (2016). The DOC algorithm has different coefficients depending on season and location (estuaries and shelf). Here the estuaries version of the algorithm was used to compute satellite DOC composites for 2003–2014 in the vicinity of the DB and CB mouths (Figures 1b and 1c).

Eight years (2007–2014) of MODIS Aqua data were processed starting with daily 1-km Level2 (L2) scenes obtained from NASA's ocean color website (oceancolor.gsfc.nasa.gov). Five years (2007–2011) were chosen to match the available concurrent ancillary data from the physical models required to compute the DOC tracer fluxes. The L2 daily remote sensing reflectances (Rrs₄₄₃, Rrs₅₄₇) were binned into Level 3 files (L3b) and then mapped and sampled for the regions of interest (L3 m). The daily L3 m 1-km reflectances were then used as input to the aCDOM₄₁₂ and DOC algorithms. About 70% of the L2 daily images had data gaps due to clouds; therefore, time series of daily DOC values at model grid points at the mouth of the bays were linearly interpolated in time to fill the gaps.

The MODIS DOC retrievals were evaluated using available data near the mouths of CB and DB (Figures 1b and 1c). Monthly time series data at stations CB8.1E, CB7.4, and CB7.4 N (see locations in Figure 1c) were

obtained from the Chesapeake Bay Program (CBP) data distribution archive (<https://www.chesapeakebay.net/what/data>). Station CB7.4 is the only one with monthly time series data concurrent with the processed MODIS data (2007–2014). A comparison between the two monthly time series revealed a bias of 21 $\mu\text{mol/L}$, with MODIS being low compared to the in situ observations; thus, the MODIS DOC at the CB mouth was adjusted everywhere by that amount before the DOC tracer flux was computed. The MODIS composites were used to extract the DOC at the locations of the in situ data and a monthly satellite climatology for each location was computed for comparison (Figure 2).

The data climatology is based on in situ observations made every month, while the algorithm climatology is based on monthly averages of the daily time series. The comparisons demonstrate good overall agreement between data and algorithm with relatively low biases (Figure 2 and Table 2). In particular, both the data and the algorithm are characterized by high values in the spring and summer compared to the fall and winter. However, variability within a given calendar month is considerably higher for the data than for the algorithm. The bias is a substantial fraction of the RMSE and thus the biases and RMSEs decreased as a result of the adjustment (Table 2).

The data available at and near the DB mouth, unlike the data from the CBP, are scattered in space and time (e.g., not time series), so two separate clusters (see Figure 1b) of stations were selected to evaluate the DOC algorithm, identified as “mouth cluster (MC)” (1980–1987, $N = 52$) and “mouth north cluster (MNC)” (1980–2006, $N = 83$). These data originate from a few different sources (Sharp et al., 2009). The evaluation of the monthly seasonal climatology between in situ data and algorithm was performed with MODIS data from 2007–2014 (Figure 3 and Table 2).

Figure 3 and Table 2 reveal that the biases in the two clusters are rather small. In fact, the bias magnitude is considerably smaller at the two DB clusters than that at the three unadjusted CB stations. However, the algorithm for DB shows distinct spring maxima that are not apparent in the data. Hence, the DB RMSEs are rather large (31 to 32 $\mu\text{mol/L}$), comparable to the RMSEs for the three unadjusted CB stations. Unfortunately, concurrent data to adjust the DB algorithm are not available.

3.4. Calculation of Uncertainties

The uncertainty on the DOC flux is calculated using the bootstrap method based on the MATLAB function “bootci,” which is the method applied to DOC fluxes in our prior study of the MAB fluxes (Mannino et al., 2016). To estimate the 95% confidence interval (CI) on the estuary mouths DOC fluxes, we applied bootstrap resampling with replacement to the satellite versus NnetM DOC percent differences (errors) for each of the estuaries to create 10,000 data sets of the errors. A probability distribution of the error was then constructed and estimates of the error (in percent) were calculated at the 2.5th and 97.5th percentiles of the corresponding probability distributions. Upper and lower bound estimates of the DOC flux were then calculated based on the error bound analysis for DOC concentrations at the 95% CI. The error on the ROMS volume transport is unknown and was therefore not accounted for in this study. For the same reason, we do not report errors for the DLEM DOC river inputs used in this study. We also accounted for the uncertainty in DOC profiles by applying a quadrature sum of squares approach for the computed MAPDs (mean absolute percent differences) of the DOC satellite algorithm and the vertical DOC profiles from the NnetM (Mannino et al., 2016). The DOC concentration uncertainty would be equal to the square root of the summed squared MAPDs from the MODIS DOC retrievals (13.9%) and the NnetM DOC profiles (7.2%), $[(13.9)^2 + (7.2)^2]^{0.5} = 15.7\%$. The total DOC flux uncertainties (95% CIs) determined by the bootstrap method shown in Table 3 account for the error between the NnetM DOC profiles and the satellite DOC.

3.5. Riverine DOC Inputs

The time series of river DOC inputs for CB and DB used in this study, and the river discharge and organic and inorganic carbon inputs (Table 1) are derived from DLEM. This is a grid cell-based, fully distributed model that couples vegetation dynamics with the cycles of water, carbon, and nutrients (Liu et al., 2012; Tian et al., 2011). The model has recently been used in eastern North America (Tian et al., 2015; Yang, Tian, Friedrichs, Hopkinson, et al., 2015; Yang, Tian, Friedrichs, Liu, et al., 2015). The basic calculation unit is a grid cell with a spatial resolution of 4×4 km and a daily time step. To account for subgrid-scale processes, the model incorporates a cohort structure, which divides each grid cell into seven land cover types: vegetation, impervious surface, glacier, lake, stream, sea, and bare ground. An improvement was made to

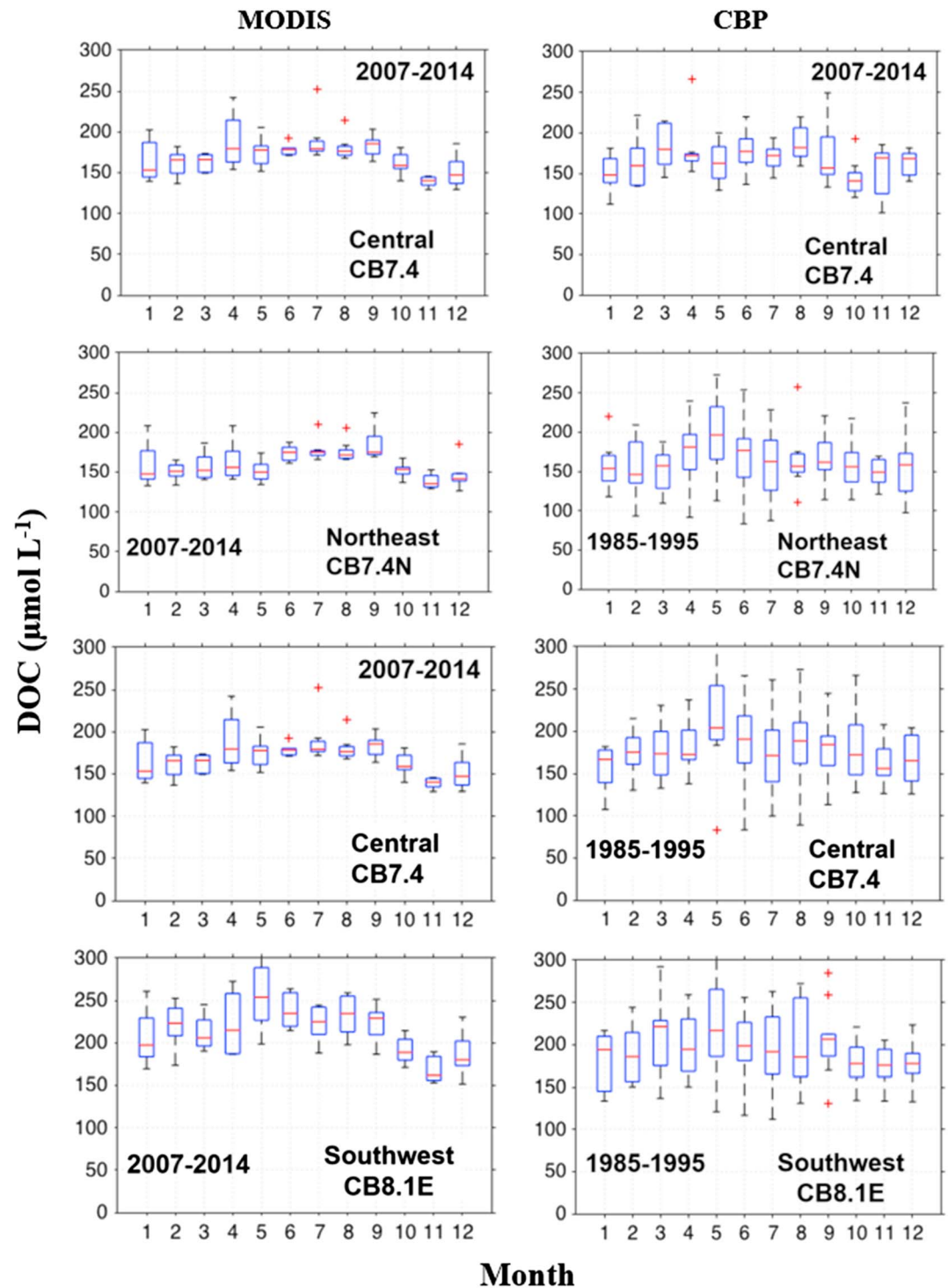


Figure 2. Box plots comparing bias-corrected MODIS DOC climatology (left column) with corresponding in situ DOC climatology from three CBP stations (right column) at the mouth of CB. The left column shows box-whisker plots of MODIS DOC for 2007–2014 and the right column Chesapeake Bay Program (CBP, 1985–1995 and 2007–2014) DOC for three stations near the CB mouth (Figure 1c). The red lines represent median values, whiskers are $\pm 2.7 \sigma$ and 99.3% coverage of the data, and the upper and lower limit of each blue box are the 75th and 25th percentile, respectively. The red crosses are outliers. The top row shows box plots of MODIS (2007–2014) and CBP (2007–2014) DOC for central station CB7.4. MODIS = Moderate Resolution Imaging Spectroradiometer; DOC = dissolved organic carbon; CB = Chesapeake Bay; CBChesapeake Bay Program.

Table 2
Statistical Summary of MODIS (M) and Observed (O) Surface DOC Mean Annual Cycles Near the Mouths of Chesapeake and Delaware Bays

Chesapeake Bay				
Period	Location	Bias	RMSE	Bias correction
1985–1995	CB8.1E	−12.5	23.8	no
	CB7.4 N	−31.4	36.4	no
2007–2014	CB7.4	−21.2	23.9	no
1985–1995	CB8.1E	8.7	18.8	yes
	CB7.4 N	−10.2	21.1	yes
2007–2014	CB7.4	0.0	11.2	yes
Delaware Bay				
Period	Cluster	Bias	RMSE	
1980–1987	MC	10.3	30.8	no
1980–2006	MNC	−11.5	32.4	no

Note. Values tabulated are bias, root-mean-square error (RMSE), and bias correction flag. The bias is defined as meanM minus meanO. All values are in $\mu\text{mol/L}$. The periods of evaluation for CB are 2007–2014 for M and 1985–1995 for O, and 2007–2014 for both M and O for station CB7.4 only. The bias of $-21.2 \mu\text{mol/L}$ at CB7.4 was used to adjust the DOC concentrations at CB mouth up by that amount before calculating the tracer flux. The periods of evaluation for DB are 2007–2014 for M and 1980–1987 for O at the mouth cluster, and 2007–2014 for M and 1980–2006 for O at the mouth north. MODIS = Moderate Resolution Imaging Spectroradiometer; DOC = dissolved organic carbon.

the hydrological components of the model to simulate riverine water and carbon pools and fluxes. Water pools in each grid cell include lake, stream, surface runoff pool, subsurface drainage pool, snowpack, and water intercepted by the vegetation canopy.

The terrestrial biogeochemical model (DLEM) accounts for climate variability. According to Yang, Tian, Friedrichs, Liu, et al. (2015), the forcings for the model are as follows: the historical daily climate data were derived from the Climatic Research Unit Timeseries (CRU TS) 2.1 data set and the NARR data set (Mesinger et al., 2006). The monthly CRU data were down-scaled to daily with daily patterns of the NARR data to make seamless combinations of these two data sets. Thus, the final climate data set contains monthly variations of precipitation and temperature from the CRU TS 2.1 data set and daily patterns from the NARR data. The reconstructed climate data time series (1901–2010) correspond well with the climate change analysis provided by the National Climate Assessment Development Advisory Committee (1901–2011). Specifically, the two data sets demonstrate similar magnitudes and spatial/temporal variability for both precipitation and temperature (Walsh et al., 2013).

3.6. DOC Production by Phytoplankton

The DOC originating from satellite retrievals within CB and DB relies on a CDOM-absorption-based algorithm fitted to in situ optical and DOC data from waters influenced by terrestrial inputs, production by phytoplankton, and transformations (e.g., remineralization and photodegradation) occurring

within the bays and nearby continental shelf. CDOM represents a portion of the bulk DOC pool, and earlier studies recognized the release of DOC by phytoplankton (e.g., Björriksen, 1988; Sharp, 1977). Many other studies addressed the DOC production by phytoplankton (Anderson & Williams, 1998; Decho & Gutierrez, 2017; Druon et al., 2010; Fisher et al., 1998; Mannino et al., 2008, 2016; Rochelle-Newall & Fisher, 2002).

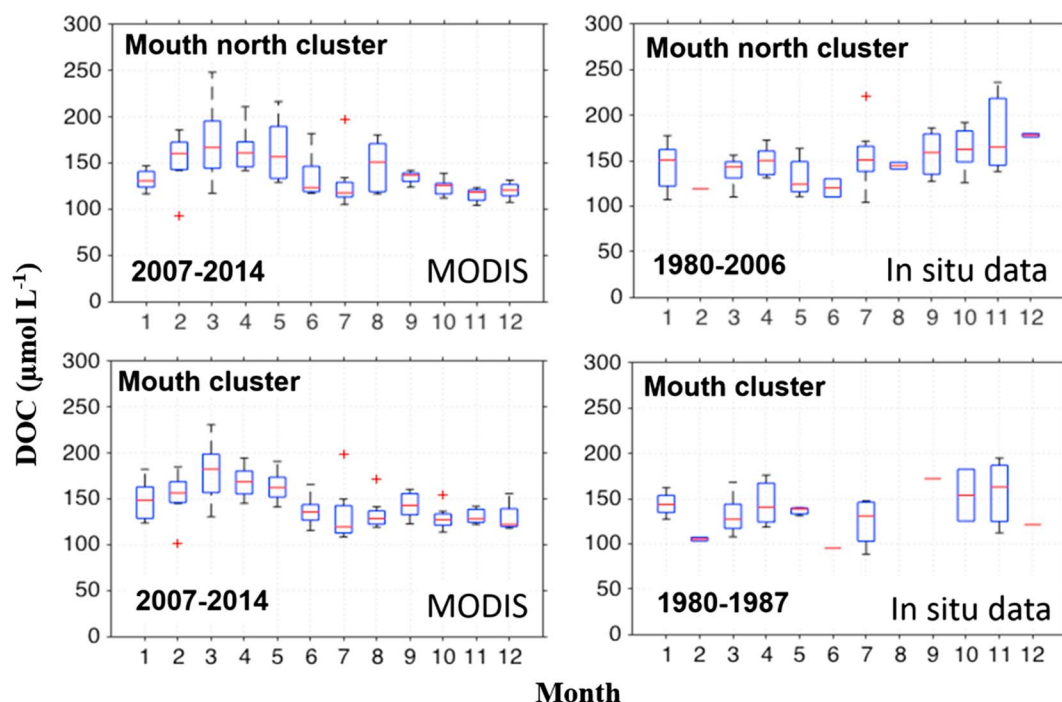


Figure 3. Box plots comparing MODIS DOC climatology (left column) with corresponding in situ DOC climatology from two cluster stations (right column) at the mouth of Delaware Bay. MODIS = Moderate Resolution Imaging Spectroradiometer; DOC = dissolved organic carbon.

Table 3

Annual Mean Values of Transect-Wide Satellite-Derived Surface Layer DOC Concentrations, Cross-Section Averaged DOC From Fully Depth Resolved DOC, Cross-Section Integrated Water Flux, Total River DOC Inputs, and Cross-Section Integrated DOC Flux at the Mouths of Chesapeake and Delaware Bays

Year	Chesapeake Bay					Delaware Bay				
	DOC conc. ($\mu\text{mol/L}$)		Water flux (m^3/s)	DOC flux (Tg C/year)		DOC conc ($\mu\text{mol/L}$)		Water flux (m^3/s)	DOC flux (Tg C/year)	
	Surface	Cross section		River	Bay mouth	Surface	Cross section		River	Bay mouth
2007	135.6	122.4	2,100	0.190	0.185 (0.100,0.286)	164.4	162.7	557	0.053	0.047 (0.020,0.076)
2008	138.6	124.0	2,602	0.203	0.181 (0.110,0.267)	161.8	160.4	562	0.066	0.038 (0.017,0.062)
2009	136.3	121.3	3,013	0.223	0.205 (0.129,0.292)	153.3	149.8	488	0.073	0.058 (0.022,0.097)
2010	151.6	136.0	2,591	0.248	0.269 (0.169,0.384)	163.1	159.5	490	0.063	0.033 (0.012,0.057)
2011	148.5	129.9	3,174	0.266	0.214 (0.135,0.307)	168.2	163.1	968	0.086	0.087 (0.051,0.125)
Mean	142.1	126.7	2,696	0.226	0.211 (0.154,0.270)	162.1	159.1	613	0.068	0.053 (0.035,0.071)

Note. The bootstrap confidence intervals are provided for the bay mouths DOC fluxes.

Both CB and DB are highly productive estuaries (Harding et al., 2002; Pennock & Sharp, 1986), so it is expected that phytoplankton blooms provide an important source of DOC to both bays.

4. Results and Discussion

4.1. Temporal Variability

Distinct differences between the DOC seasonal cycles of the CB and DB (Figure 4) can be in part accounted for due to their distinct physical and biogeochemical attributes (Table 1). In CB, the 5-year mean seasonal cycle shows a broad peak in DOC concentrations during July–September. In DB there are peak DOC values in March and October and a minimum value in July. The mean seasonal DOC range (maximum minus minimum) is around $30 \mu\text{mol/L}$ in CB and $50 \mu\text{mol/L}$ in DB. There are also distinct differences between the seasonal cycles of DOC flux at the two bay mouths. The most obvious is the large difference in the DOC flux magnitude (positive, representing net export out of the bays), with CB being larger due to a factor of ~ 4 greater freshwater input when compared to DB (Figure 4). Both CB and DB show DOC flux maxima in spring and minima in fall.

There is a large interannual variability in the integrated water flux across the mouths of both bays, mainly due to variability in the freshwater inputs (see Table 3 and Figure S2 in the supporting information). For example, in the CB, the mean annual water flux (net out of the bay) was 51% greater in 2011 than 2007. In DB, the mean annual water flux in 2011 ($968 \text{ m}^3/\text{s}$) was almost doubled that of 2009 ($488 \text{ m}^3/\text{s}$). These substantial interannual differences are evident from the large standard deviations in the 2007–2011 monthly water flux climatology from CB and DB (Figures 5 and 6).

These large interannual changes of water flux have a significant impact on the variability of the integrated DOC tracer flux at both bay mouths, as shown in Table 3. In CB, the net annual outgoing DOC flux was $\sim 30\%$ greater in 2010 than in 2007. The variability in the annual mean outgoing DOC flux was more significant in DB where the flux was 2 times greater in 2011 than in 2010. The variability in the water flux across the bay mouths was the driving factor in the interannual differences in DOC fluxes (Table 3).

The mean water volume and DOC fluxes from the estuary to the ocean are much larger for CB than for DB, in agreement with the much larger input of freshwater to CB compared to DB (Table 3). The CB/DB ratio of water export (leaving) flux is 4.4, while the equivalent ratio of DOC export flux at the bay mouths is very similar (4.2). A rough estimate of the DOC flux at the bay mouths is the product between the long-term mean (2007–2011) cross section-averaged DOC concentration and the long-term mean integrated water flux across the bay mouths (Table 3), which are calculated as 0.129 Tg C/year and 0.037 Tg C/year for CB and DB, respectively. These estimates are 39% and 30% too low when compared with the values obtained from the complete convolution of the two time series.

These underestimates indicate a covariation (temporally, spatially, or both) in water flux and DOC concentration at each of the bay mouths. The covariation contributions to the flux can be determined by decomposing the DOC concentration C and the velocity perpendicular to the mouth transect u into components that are constant in space, constant in time, and vary in space and time (but have zero means). Let $f = uC$ be the

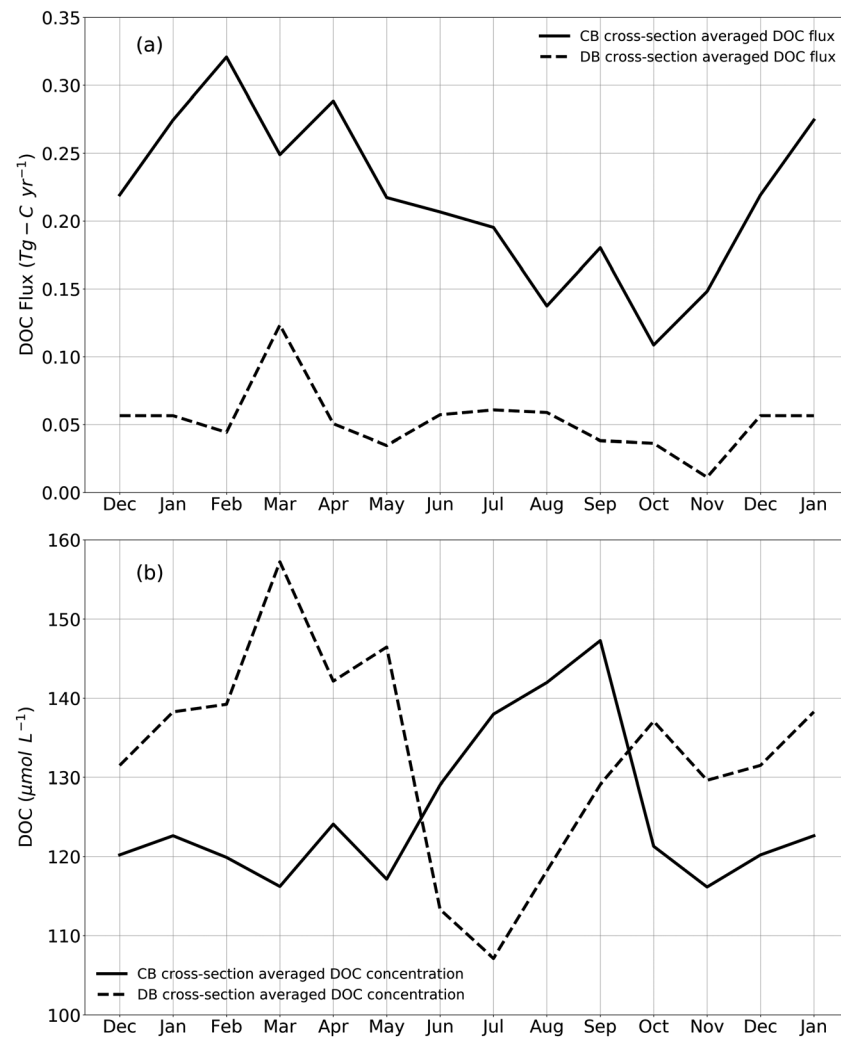


Figure 4. Monthly 5-year (2007–2011) seasonal plots of cross-section averaged DOC flux (a) at the mouths of CB and DB, and equivalent cross-section averaged DOC concentration (b). DOC = dissolved organic carbon; CB = Chesapeake Bay; DB = Delaware Bay.

fully resolved flux in space and time, which has units of $mmol C \cdot m^{-2} \cdot s^{-1}$. Then, according to standard flux decomposition (Lerczak et al., 2006; Peixoto & Oort, 1992) the spatially averaged flux across the transect is

$$\langle f \rangle = \langle u \rangle \langle C \rangle + \langle u^* C^* \rangle \quad (4)$$

where $\langle \rangle$ indicates the spatial average and $*$ indicates the deviation from the spatial average. The time average of equation (4) is

$$\overline{\langle f \rangle} = \overline{\langle u \rangle} \overline{\langle C \rangle} + \overline{\langle u \rangle' \langle C \rangle'} + \overline{\langle u^* C^* \rangle} \quad (5)$$

where the overbar indicates the long-term temporal average (5 years) and $'$ indicates the deviation from the temporal average. The first term on the right-hand side of equation (5) represents the DOC flux resulting from the long-term mean DOC concentration and mean water flux at the bay mouth. The second term reflects the DOC flux due to temporal covariation of the spatial mean DOC concentration with the spatial mean velocity. The third term reflects the DOC flux due to spatial covariation of the DOC concentration with the water flux. The analysis was conducted using daily time series data. The long-term (5-year) mean values of all three decomposition terms (after multiplying by cross-sectional area), along with the water flux, DOC concentration, and fully resolved DOC flux, are provided in Table 4 for DB and CB. The spatial and temporal

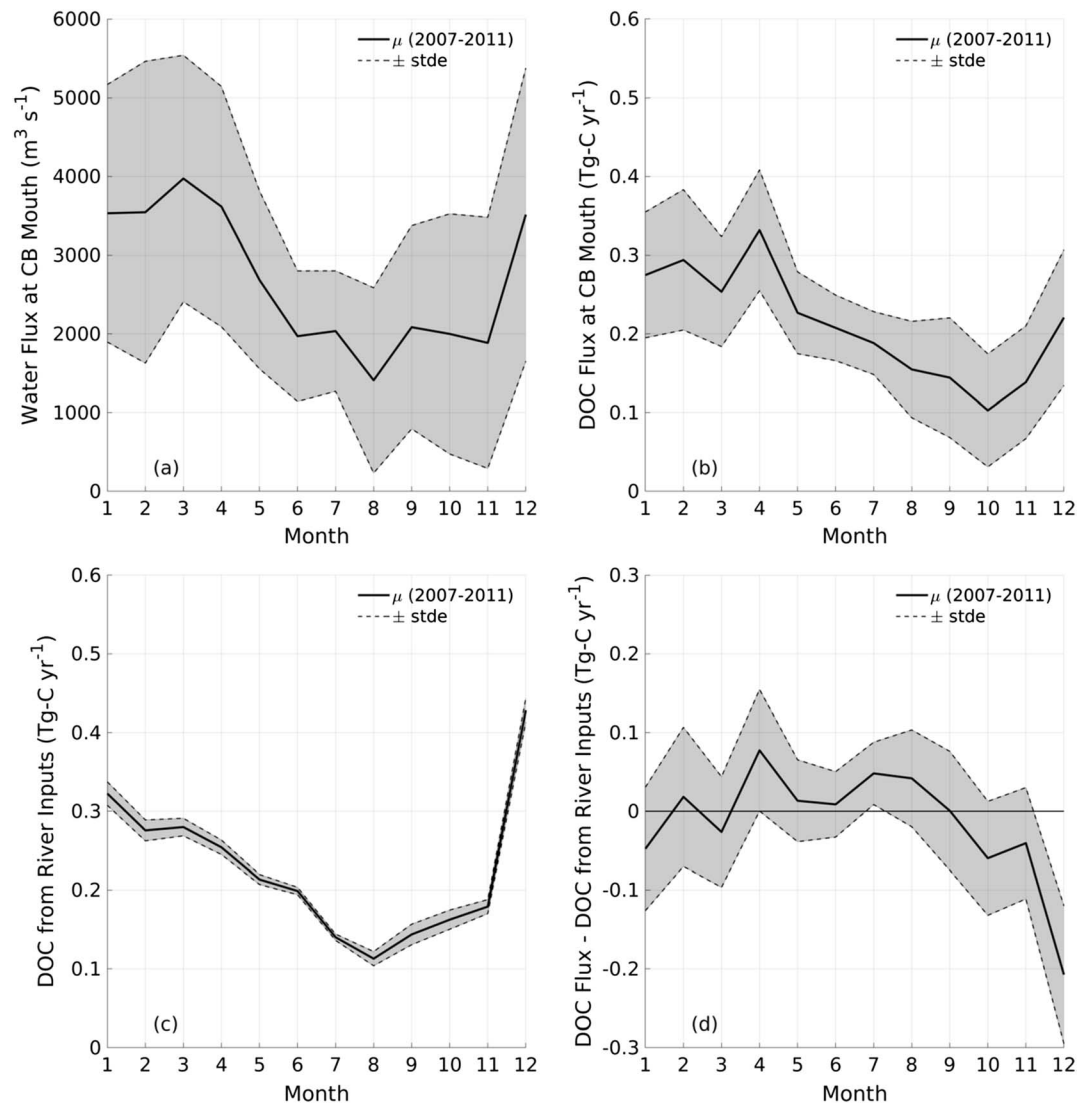


Figure 5. Cross-section integrated seasonal water flux (a) and DOC flux (b) at CB mouth, DOC inputs from rivers (c), and the difference between the DOC flux and river DOC inputs (d). Seasonal plots and mean values are shown for the overall 5-year averages (thick black line). The lines bounding the gray-shaded areas correspond to ± 1 standard error. The term μ refers to the 5-year mean, and stde represents the standard error. DOC = dissolved organic carbon; CB = Chesapeake Bay.

covariations in the DOC flux (Table 4) play an important role in the estimates of DOC export in both bays, with the spatial deviations having a relatively stronger importance, especially in CB. In DB, the temporal covariations are substantial; they represent 13% of the mean DOC flux. In contrast, the temporal covariations play a negligible role in CB; they represent only 1% of the mean DOC flux. The much larger temporal covariations in DB are likely a result of the greater influence of tides in DB compared to CB. The importance of the spatial covariations will be discussed in section 4.2.

The positive peak in April in CB DOC $E-R$ (difference in DOC export at the bay mouth minus riverine inputs of DOC of the bay) suggests that the export of DOC produced/transformed within the bay exceeds the DOC river inputs, while the opposite occurs during the fall–winter period when $E-R$ is negative (Figure 5). However, completion of the balance requires the time rate of change of DOC in the estuary, inputs from wetlands, and inputs from sediments, which were not estimated in the present study. The seasonality of $E-R$ for DB is similar (Figure 6), albeit with much smaller values, which are a result of significant lower cross-section water flux as a consequence of the lower freshwater inputs into the bay. Long-term means of riverine DOC

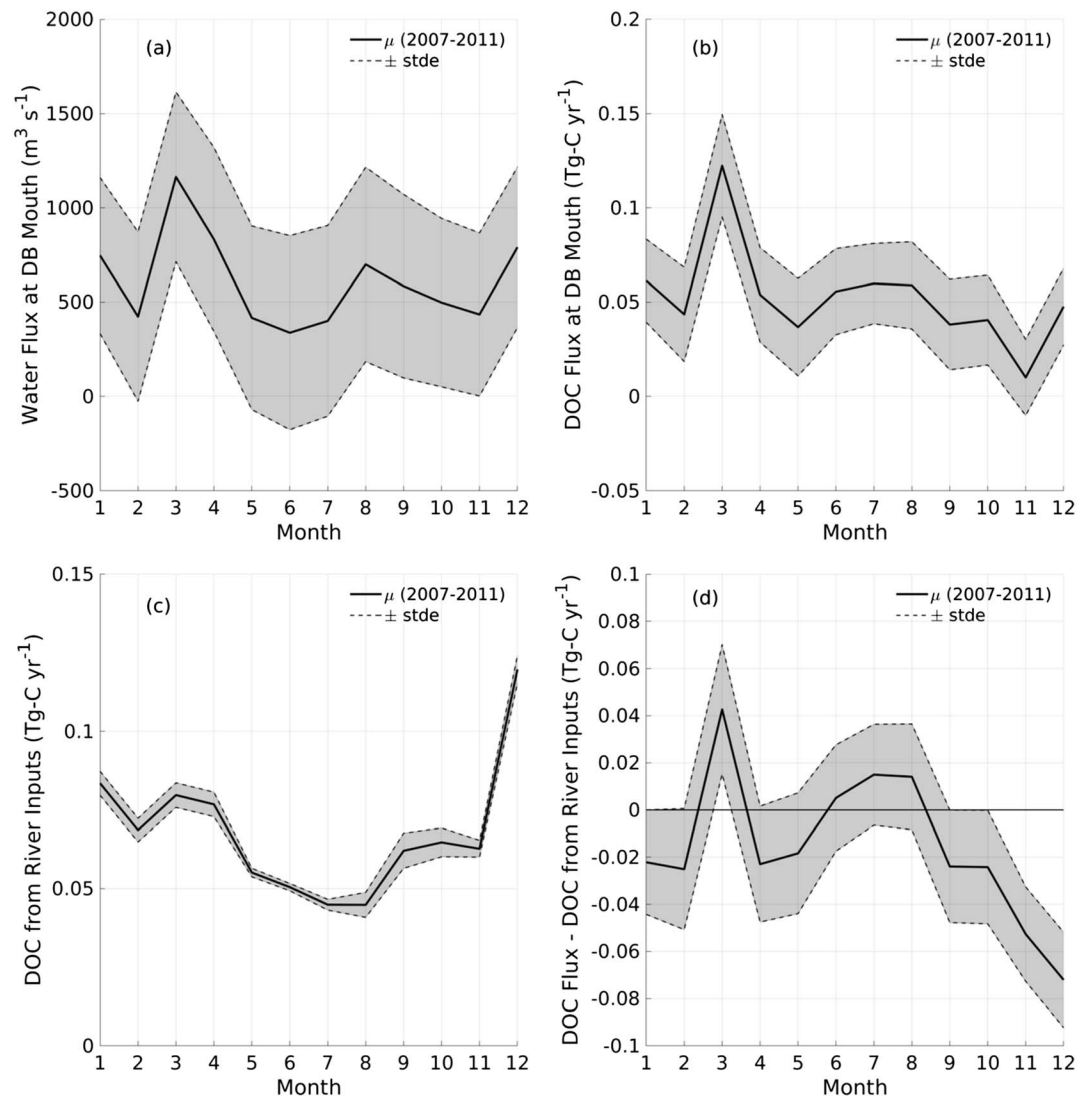


Figure 6. Cross-section-integrated seasonal water flux (a) and DOC flux (b) at DB mouth, DOC inputs from rivers (c), and the difference between the DOC flux and river DOC inputs (d). Seasonal plots and mean values are shown for the overall 5-year averages (thick black line). The lines bounding the gray-shaded areas correspond to ± 1 standard error. The term μ refers to the 5-year mean, and stde represents the standard error. DOC = dissolved organic carbon; DB = Delaware Bay.

input are only slightly higher than DOC export at the bay mouths (Table 3), suggesting an overall balance between remaining DOC sources (e.g., from marshes, sediments, and primary production) and DOC sinks (e.g., bacterial consumption and photochemical oxidation).

Interannual variability in DOC export from CB and DB is significant. For example, the largest peak in DOC river inputs and DOC export occurred during winter–spring 2010 in CB, most likely due to a delayed impact of the remnants of Hurricane Ida during 10–14 November 2009, which contributed to the emergence of an extratropical cyclone that brought heavy rainfall and gusty winds to the CB watershed. Both DOC river inputs and DOC export out of the bay reached 0.6 Tg C/year in January 2010, about 3 times the 5-year averaged DOC export out of the bay reported in this study. During 7–10 September 2011, the remnants of Tropical Storm Lee moved across Maryland causing widespread flooding, particularly in the western portion of the state. In combination with the impact of Hurricane Irene, which occurred earlier on 27 August 2011 and caused hurricane conditions to the east of CB, rainfall totals reached up to 61 cm of rain in the region. In late 2011, the total river DOC inputs reached nearly 0.5 Tg C/year and close to 0.4 Tg C/year DOC export out

Table 4

Summary of 5-Year (2007–2011) Averages of All Terms in Equation (5), Where \overline{f} is the Fully Resolved Flux in Space and Time, $\langle u \rangle \langle C \rangle$ is the DOC Flux Resulting From the Long-Term Mean DOC Concentration and Mean Water Flux at the Bay Mouth, $\langle u' C' \rangle$ is the DOC Flux Due to Temporal Covariation of the Spatial Mean DOC Concentration With the Spatial Mean Velocity, and $\langle u^* C^* \rangle$ is the DOC Flux Due to Spatial Covariation of the DOC Concentration With the Water Flux

Terms in equation (5)	Covariation	Chesapeake Bay	Delaware Bay	Units
\overline{u}		0.0126	0.0027	m/s
\overline{C}		123.0	130.2	mmole C/m ³
\overline{f}^*A		0.211	0.053	Tg C/year
$\langle u \rangle \langle C \rangle^*A$	Long-term mean	0.125	0.030	Tg C/year
$\langle u' \rangle \langle C' \rangle^*A$	Temporal	0.0045	0.0083	Tg C/year
$\langle u^* C^* \rangle^*A$	Spatial	0.0812	0.0140	Tg C/year

Note. The flux decomposition terms in the last four rows were multiplied by the cross-section area and converted to Tg C/year.

of the bay. Other storms, when combined with the spring freshet, also caused an impact on the fluxes shown with somewhat lesser impact in DB.

The evidence suggests that episodic events such as storm events and high-frequency pulses of water and DOC export from tidal exchange play an important role in the flux of DOC from the CB and DB (see daily time series in Figure S1 in the supporting information).

4.2. Spatial Variability

The long-term mean (2007–2011) DOC, velocity, and DOC flux transects across the mouths of CB and DB show significant horizontal and vertical stratification (Figure 7). The bathymetry across the bay mouths shows distinct differences (Figures 1b and 1c), which have an impact on the spatial variability of DOC concentrations and DOC flux. The DB mouth is deeper than that of CB on average and has a distinct deeper and narrower channel on the southeast side that leads to the canyon offshore (see Figure 1c). The DOC plume exiting DB is relatively narrow with DOC concentrations peaking at more

than 175 $\mu\text{mol/L}$ and confined to the south side of the deep channel. The CB DOC plume is much broader (~ 7 km at the surface in summer) with DOC concentrations peaking on the southern side of the mouth at nearly 200 $\mu\text{mol/L}$. The intrusion of marine DOC is identified near the bottom where the lowest values (95–100 $\mu\text{mol/L}$) occur. The DOC plume region in CB shows stronger vertical stratification when compared to DB (the plume is nearly vertically homogeneous), consistent with expectations of the different physics of the two estuaries (section 2). The averaged transects of DOC fluxes (Figure 7) indicate that there is more variability in the flux across the mouth in DB than in CB. In CB, DOC flux at the bay mouth is characterized by export that peaks at the surface and near the southern transect end. In contrast, import is concentrated at the southern and northern transect ends and tends to be more vertically uniform, though highest values are typically at depth. In DB, there is a narrow (4 km) jet flowing out of the bay in the southeastern corner of the mouth. The remaining portion of the transect to the northeast shows weaker fluxes that vary in sign (direction), except near the northeast end where there is a strong and narrow inflow jet of about 2 km in width.

Spatial covariations between DOC concentration and water flux (third term in equation (5)) play an important role in the accurate representation of DOC export (Table 4). Figure 7 clearly shows that both bay mouths have significant transect-wide spatial variability in DOC concentration and DOC flux. For example, Table 4 shows that in CB spatial covariations play a major role (0.0812), which is nearly as large as cross-section-averaged flux (0.125). Inspection of Figure 7 reveals that these spatial covariations between DOC concentrations and the flux occur vertically and horizontally across the bay mouth.

An estimate of the DOC flux can be computed by multiplying the transect-averaged DOC by the mean outgoing water flux. For example, using the CB values for 2011, the wettest year of the 5-year period, and applying the proper conversion factors, one gets a DOC export of 0.16 Tg C/year, which is $\sim 24\%$ lower than the 0.21 Tg C/year calculated using the tracer flux methodology applied in this study. The same calculation for DB results in a value of 0.06 Tg C/year, which is a 33% underestimate when compared to the 0.09 Tg C/year using the tracer flux method. This shows that, to achieve more accurate estimates of DOC export, we must take into account the spatial and temporal complexity of the DOC concentrations and water volume exchange across a given transect (see Table 4). This requires extensive efforts by field, modelers, and remote sensing scientists.

Regarding the impact of the bias correction on the DOC flux, the temporal variability will be affected by an offset only. The magnitude of the mean flux across CB mouth for 2007–2011 is reduced by about 10% without the bias correction (from 0.21 to 0.19 Tg/year). This seems like a small reduction as the 21 $\mu\text{mol/L}$ adjustment accounts for 40% of the seasonal variability at CB mouth. However, the flow across CB mouth, as shown in Figure 7b, is not vertically uniform, in fact it changes direction from out of the bay in the upper depths within the plume to into the bay below the plume, which provides a compensating effect for changes in DOC concentrations uniformly across the mouth. Changes in the vertical DOC stratification and changes

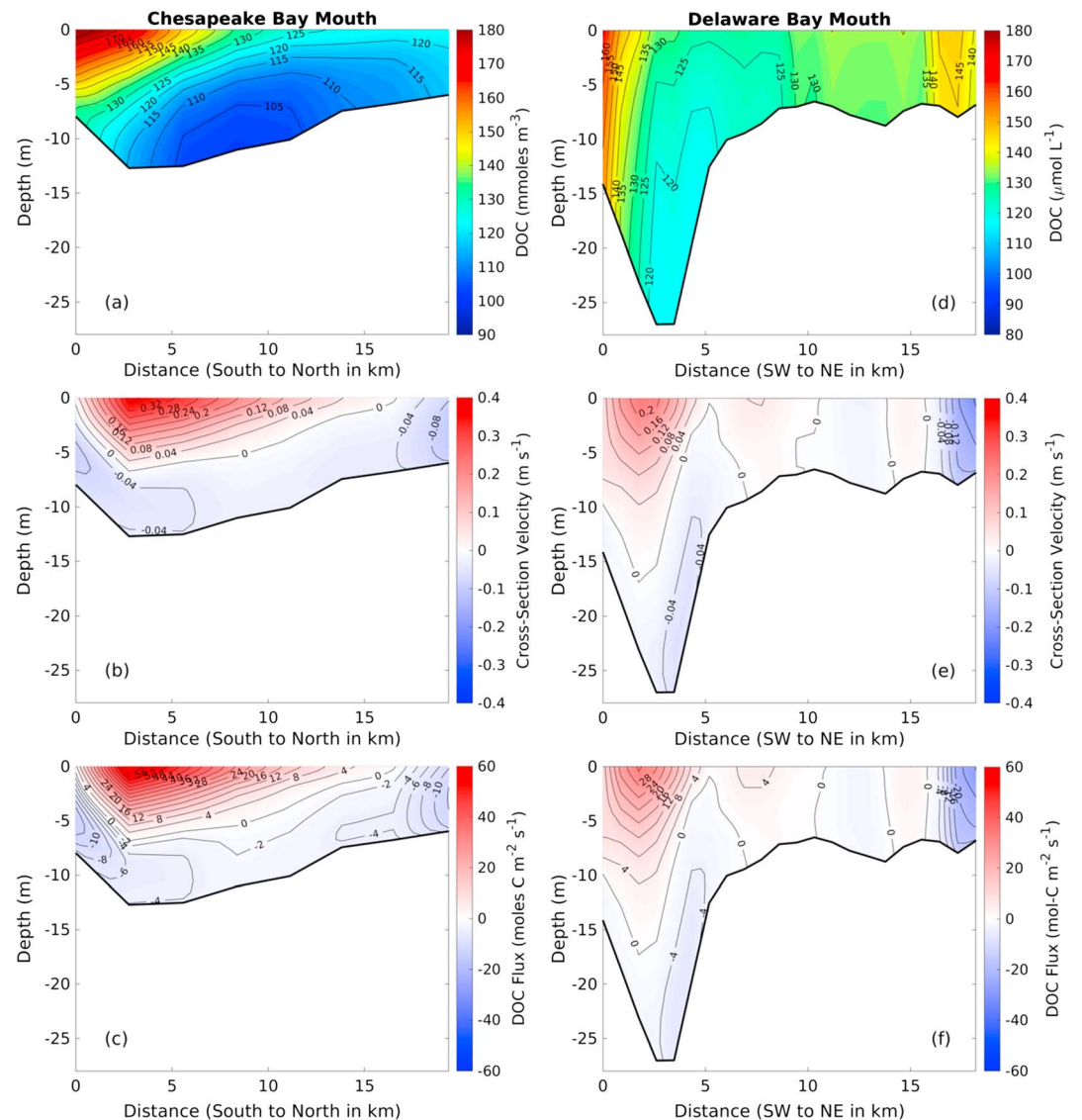


Figure 7. Five-year averaged cross sections of DOC concentration, velocity, and DOC flux at the mouths of Chesapeake Bay (a–c, respectively) and Delaware Bay (d–f, respectively). DOC = dissolved organic carbon.

in the water flow spatial variability, a dominant factor in the DOC flux determination, are more influential in the estimate of the DOC export from the bays.

4.3. Terrestrial Versus Marine DOC

On a month-to-month basis there are relatively large alternating positive and negative deviations (gray-shaded areas) between the terrestrial DOC inputs (DLEM total river inputs) and the DOC exported at the mouths of the estuaries (Figure 8), indicating changes in the DOC inventories in the estuaries, other external sources (e.g., tidal wetlands and groundwater), and estuarine internal sources and sinks of DOC. Here we discuss the internal sources and sinks. The biochemical composition of terrestrial and marine DOC in CB and DB is influenced by reactive transformations (Mannino & Harvey, 2000a, 2000b). For instance, in DB riverine DOC is transformed (i.e., remineralized), and autochthonous DOC is introduced into the bay (Mannino & Harvey, 2000a). Mannino and Harvey (2000b) showed that terrestrial DOM (lignin) in the high molecular weight pool is exported from DB at a rate of 0.02 Tg C/year. DOC does not mix conservatively in DB; instead, transformations of DOC from river to sea result in losses of terrestrial DOC with concurrent contributions of autochthonous DOC (Harvey & Mannino, 2001). Similar transformations occur in CB

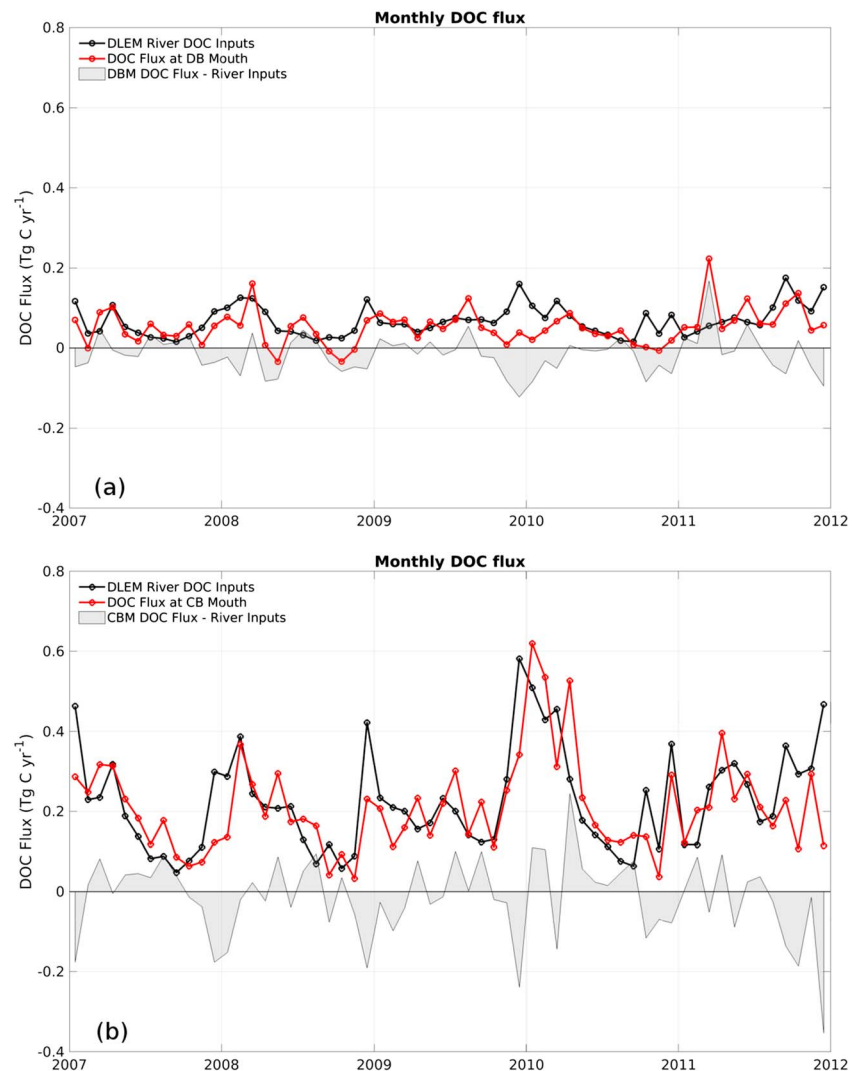


Figure 8. Monthly time series of Dynamic Land Ecosystem Model (DLEM) total river DOC inputs, Sat-NNet DOC tracer flux at the bay mouths (DOC export), and the difference between export DOC and river inputs for DB (a) and CB (b). DOC = dissolved organic carbon; DB = Delaware Bay; DBM = Delaware Bay mouth; CB = Chesapeake Bay.

including autochthonous production of DOC during periods of nutrient limitation in bay waters (Rochelle-Newall & Fisher, 2002). For instance, there is a net accumulation of DOC (net community production) by nutrient-limited phytoplankton production within CB (Fisher et al., 1998).

Although it is difficult to quantitatively separate the DOC of terrestrial origin from the DOC of marine origin in such complex estuarine systems, which include DOC of riverine origin, DOC from wetlands, and DOC produced within the bays and in the nearby shelf region, a qualitative assessment can be made based on spectral characteristics of terrestrial versus marine CDOM. For instance, CDOM spectral slope (and CDOM concentration) can be used as a relative measure of terrestrial versus autochthonous DOM (Blough & Del Vecchio, 2002; Helms et al., 2008). In general, terrestrial CDOM has smaller spectral slopes of CDOM absorption coefficient than marine CDOM, and it is, in general, associated with higher values of DOC. Using this CDOM versus DOC distinction, the concurrent variations of spectral slope and DOC concentrations can be analyzed in an attempt to qualitatively construct a type of end-member mixing diagram for terrestrial versus marine DOC. To that end, two clear Level-2 MODIS scenes were selected covering most of CB and DB, from 28 April and 23 September 2004, which represent relatively high- and low-flow conditions, respectively. We then processed the images using the CDOM/DOC MLRC algorithm to derive three

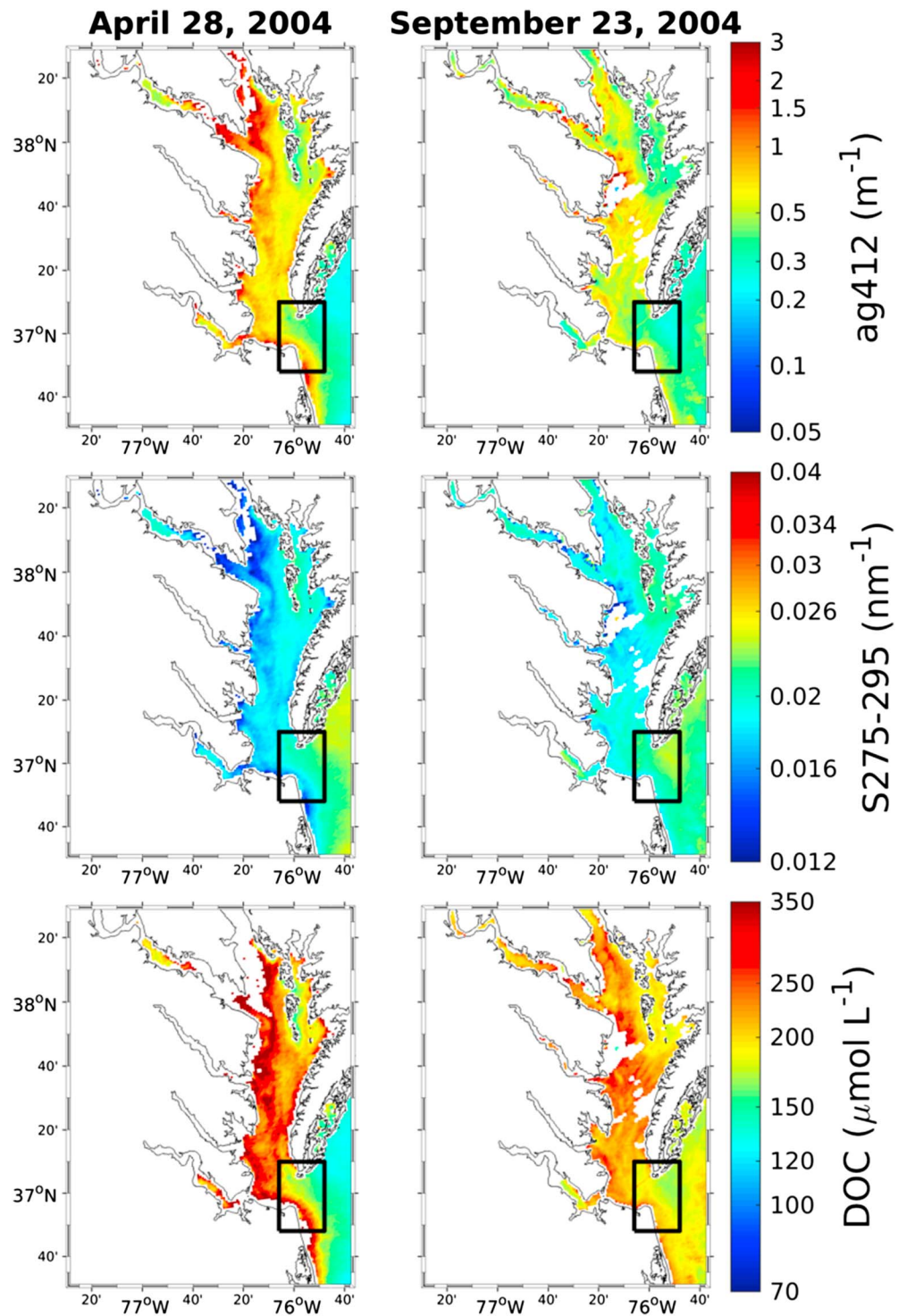


Figure 9. MODIS images of Chesapeake Bay CDOM absorption coefficient at 412 nm (ag_{412} ; top row), CDOM spectral slope between 275 and 295 nm ($S_{275-295}$, middle row), and DOC (bottom row) for 28 April and 23 September 2004. The rectangular areas are regions within the bay mouths for statistical analysis (see Figure 11). MODIS = Moderate Resolution Imaging Spectroradiometer; CDOM = chromophoric dissolved organic matter; DOC = dissolved organic carbon.

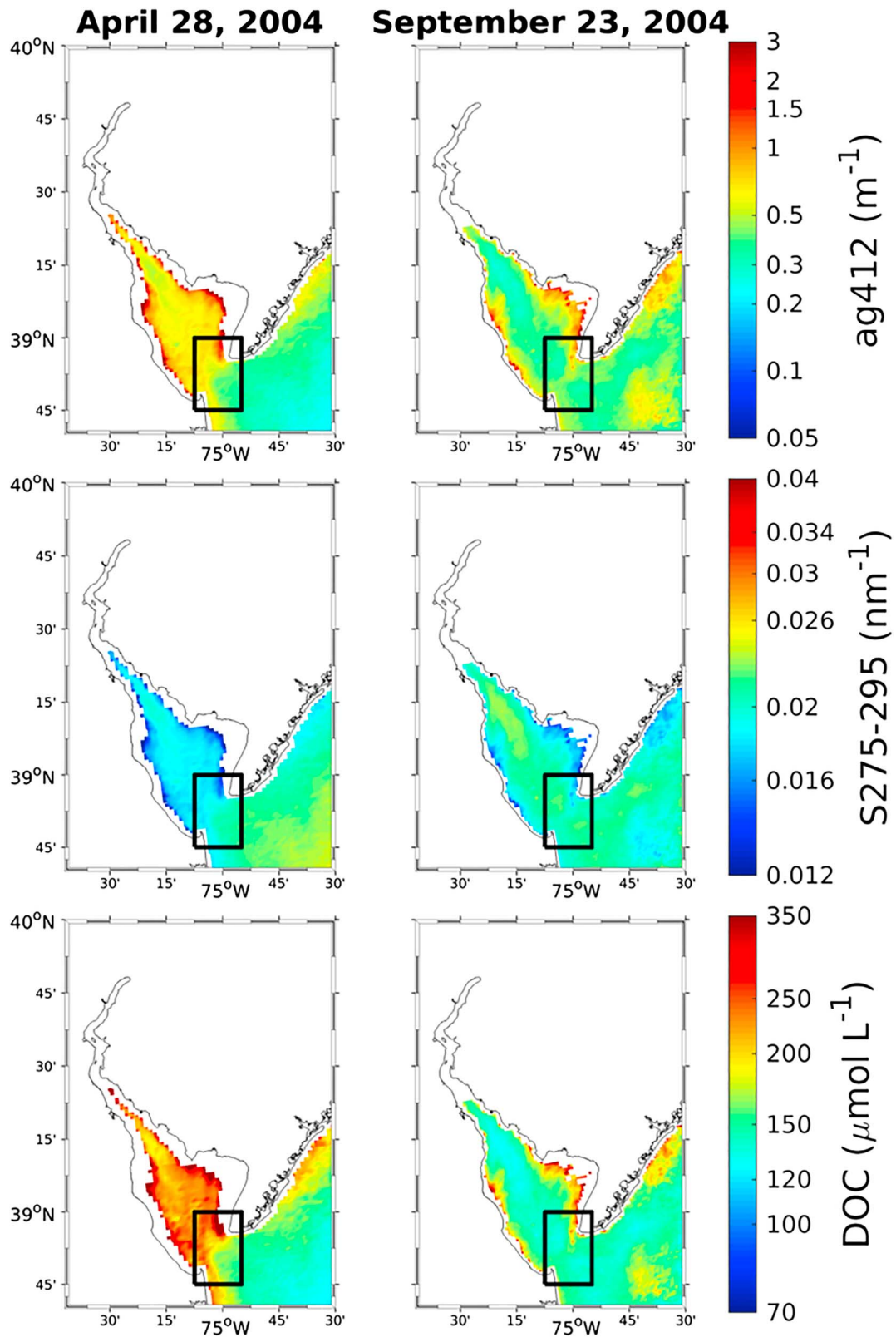


Figure 10. MODIS images of Delaware Bay ag412 (top row), s275–295 (middle row), and DOC (bottom row) for 28 April and 23 September 2004. The rectangular areas are regions within the bay mouths for statistical analysis (see Figure. 11). MODIS = Moderate Resolution Imaging Spectroradiometer; DOC = dissolved organic carbon.

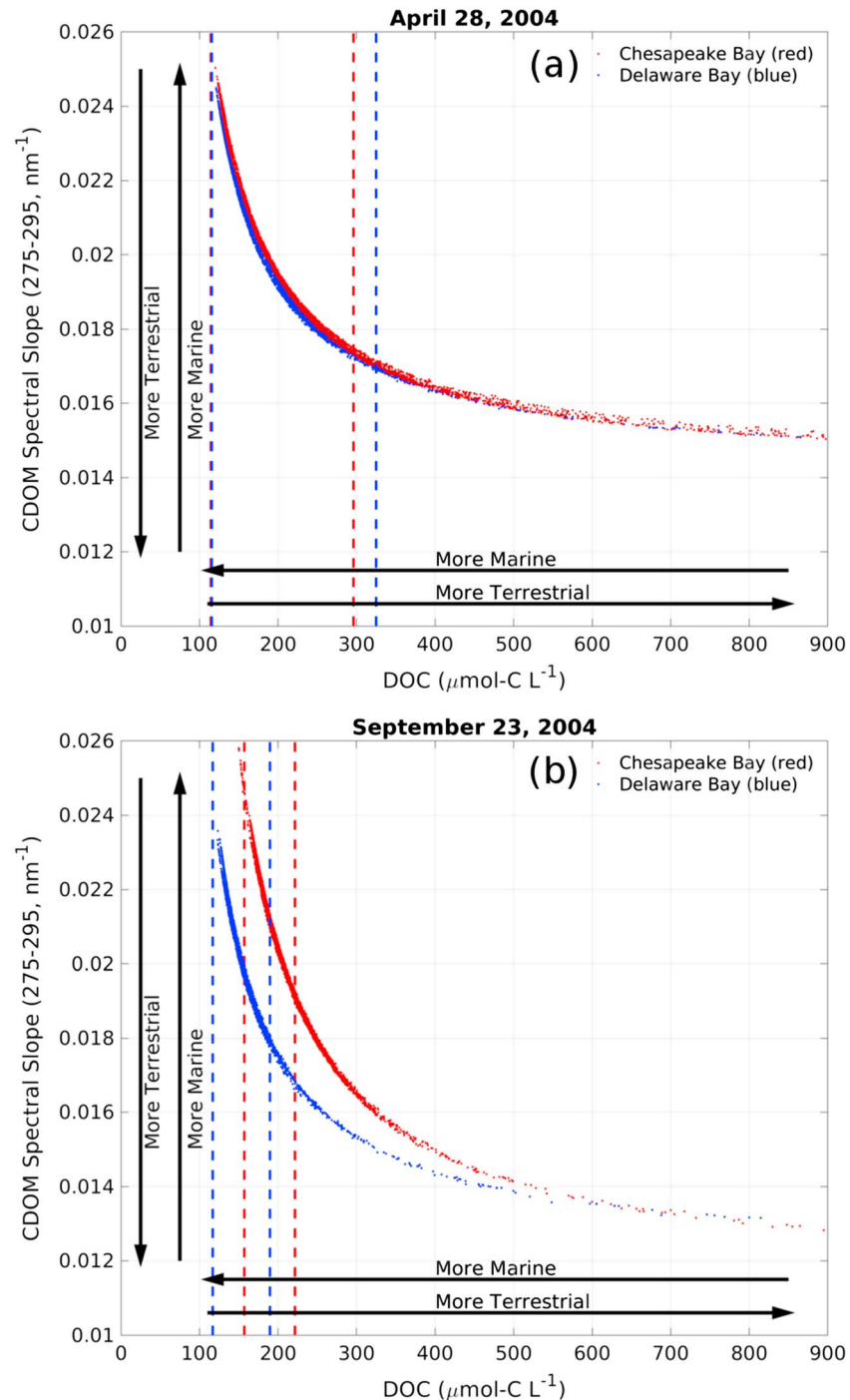


Figure 11. Diagrams of DOC versus CDOM spectral slope for 275–295 nm spectral range, CB (red) and DB (blue). The top panel derives from the 28 April 2004 image and the bottom panel from 23 September 2004. The black arrows point to the terrestrial and marine end members on the diagram. The vertical dashed lines represent the mean DOC $\pm 1\sigma$ within the bay mouths (rectangular areas in Figures 9 and 10). Only surface DOC and CDOM spectral slope were used in the analysis. DOC = dissolved organic carbon; CDOM = chromophoric dissolved organic matter; DB = Delaware Bay; CB = Chesapeake Bay.

products, ag_{412} (CDOM absorption coefficient at 412 nm), spectral slope of the CDOM absorption coefficient for 275 to 295 nm ($S_{275-295}$), and DOC (Mannino et al., 2016).

The MODIS CDOM and DOC data products from 28 April and 23 September 2004 for CB and DB provide some insight on the spatial and seasonal contributions of terrestrial and marine DOC (Figures 9 and 10, respectively). The April image depicts the peak of the terrestrial DOC inputs to the bays from river discharge so that ag_{412} and DOC concentrations are high within the bays, while the CDOM absorption spectral slopes ($S_{275-295}$) are relatively low. In contrast, the September image shows much lower ag_{412} and DOC, and relatively higher values of $S_{275-295}$, an indication of reduced terrestrial DOC inputs and more DOC produced within the bays. The boxes on the images represent the regional domains of the bay mouths (CBM and DBM) that contain our study areas. Note that the September DOC concentrations in CBM are higher than in DBM, despite having similar ag_{412} and $S_{275-295}$ values. Relative proportions of terrestrial and marine DOC are represented by end-member mixing diagrams (Figure 11) that are based on scatter plots of DOC versus $S_{275-295}$ using image pixels from the CB and DB images shown in Figures 9 and 10. The range of DOC for the bay mouth study area defined in Figures 9 and 10 was wider in April during the highly variable terrestrial DOC inputs during the preceding winter–spring period, and much narrower during September when terrestrial inputs decrease significantly and local (autochthonous) production increases during the late summer period. Mixing proportions of terrestrial and marine DOC cannot be directly derived from these diagrams (shown in Figure 11), but they provide a graphical illustration of how dynamic and reactive these estuaries are to biogeochemical and photochemical changes (Del Vecchio & Blough, 2004). The higher DOC and $S_{275-295}$ pattern for CB in September compared to DB can be attributed to greater autochthonous production within CB during the summer period than in DB (Fisher et al., 1998; Mannino et al., 2008).

5. Summary and Conclusions

We adopt a novel method to quantify the estuary-ocean exchange of DOC for two coastal plain estuaries, Chesapeake Bay and Delaware Bay. The method relies on high-frequency (daily) estimates of satellite-derived DOC concentration and water flux obtained from a hydrodynamic model, and a neural net model trained with in situ data to extend the DOC satellite retrievals into vertically resolved DOC concentrations. This assessment of estuary-ocean DOC exchange captures vertical, horizontal, and temporal (daily over the 2007–2011 period) variability in the exchange. The results are compared with DOC riverine inputs computed from a terrestrial biogeochemical model to help interpret the large temporal variability observed in the 5-year assessment.

The 5-year mean DOC flux for CB and DB are 0.21 (0.15, 0.27) Tg C/year, and 0.05 (0.04, 0.07) Tg C/year, respectively. A flux decomposition analysis showed that temporal and spatial covariations in the DOC flux at the mouth of both bays play a significant role in determining the net export of DOC from the estuaries, which suggests that accurate estimates of estuarine DOC export requires information on scales that properly resolve the temporal and spatial variability of water flux and DOC concentration. Neglecting these temporal and spatial covariations in the DOC flux leads to a 40% underestimation of the DOC flux in CB and 28% in DB.

For the 5-year (2007–2011) average, the total river DOC inputs in each estuary are very close to their respective DOC export out to the shelf. However, CB and DB are not pipes, but rather transformers or reactors (e.g., terrestrial DOC is mineralized and allochthonous DOC is produced), so, after undergoing transformations, the DOC exported from the bays is a combination of terrestrial DOC and estuarine DOC. In fact, on a month-to-month basis there are relatively large alternating positive and negative deviations between the terrestrial DOC (riverine) inputs and the DOC exported at the mouths of the estuaries, indicating seasonal changes of the DOC transformation processes within the estuaries.

These high-frequency estimates of DOC fluxes from CB can help us understand the estuarine organic carbon subsidy to continental shelves for use by the microbial community as well as improve carbon budgets for the estuaries and continental shelf. In addition, the method of using model flow fields enables making a thorough estimate of the flow and thus the DOC flux at the mouths of the estuaries, which are difficult to accomplish with in situ direct current measurements due to the logistical challenges that it imposes.

Recent mass balance method studies (Crosswell et al., 2017; Herrmann et al., 2015; Najjar et al., 2018) on estuary-ocean exchange of carbon demonstrate the importance of this exchange in estuarine carbon budgets and its dependence on estuarine net ecosystem production, CO₂ exchange with the atmosphere, and burial. Estuary-ocean exchange of carbon and related quantities (e.g., nutrients, oxygen, and alkalinity) is thus not only important for understanding the land-ocean link in global biogeochemical cycles but is an important metric of biogeochemical processing within an estuary (Feng et al., 2015). The absence of direct determinations of this important carbon flux is unfortunate, particularly in light of the large changes that the coastal zone is undergoing in response to climate and land use change. The present study provides improved understanding and closes the gap in our knowledge of the processes contributing to estuary-ocean exchange of carbon.

The combined export of DOC from CB and DB based on the 5-year averages is 0.3 Tg C/year. Based on previous estimates of total organic carbon (TOC) exported by all MAB estuaries (1.2 Tg C/year), and all East Coast estuaries combined (3.4 Tg C/year; Herrmann et al., 2015), the DOC export of 0.3 Tg C/year estimated here corresponds to 25% of the TOC exported by all MAB estuaries, and 9% of the TOC exported by all East Coast estuaries. Therefore, CB and DB play a significant role in the overall coastal budget of organic carbon. Furthermore, based on estimates of air-sea CO₂ flux for the MAB (Signorini et al., 2013), the combined CB and DB DOC export is about 27% of the 1.1 Tg C/year air-sea CO₂ uptake in the MAB, a major contributor to the total carbon budget for the shelf region.

The work conducted in this study is part of a larger ongoing effort from our group to develop a carbon budget for the MAB and Gulf of Maine (including the major estuaries) using a combination of coupled terrestrial, estuarine, and oceanic physical-biogeochemical models that include the environmental impact of climate change. Recent studies highlight the importance of the environmental impact of warming and CO₂ increase in the land-estuarine-ocean boundaries (Brewer, 2018; Reimer et al., 2017), which is a relevant topic of interest to be addressed in our future studies.

Acknowledgments

We want to acknowledge the NASA Interdisciplinary Science Program (USECoS Project, grants GSFC SCMD-Earth Science System_ 509496, NNX11AD47G, and NNX14AF93G) and the Ocean Biology and Biogeochemistry Program (ClIVEC; GSFC SCMD-Earth Science System_444491) for supporting this work. R. G. N. also recognizes support from the WETCARB project (NASA grant NNX14AM37G). This paper is contribution 3820 of the Virginia Institute of Marine Science, William & Mary. All the data and model output in the figures can be downloaded from the Open Science Framework (<https://osf.io/czfk4/>) data archive.

References

- Amann, T., Weiss, A., & Hartmann, J. (2015). Inorganic carbon fluxes in the inner Elbe estuary, Germany. *Estuaries and Coasts*, 38(1), 192–210. <https://doi.org/10.1007/s12237-014-9785-6>
- Anderson, T. R., & Williams, P. J. B. (1998). Modelling the seasonal cycle of dissolved organic carbon at Station E1 in the English Channel. *Estuarine, Coastal and Shelf Science*, 46(1), 93–109. <https://doi.org/10.1006/ecss.1997.0257>
- Axelrad, D. M., Moore, K. A., & Bender, M. E. (1976). Nitrogen, phosphorus, and carbon flux in Chesapeake Bay marshes. Retrieved from Blacksburg, Virginia.
- Bauer, J. E., & Bianchi, T. S. (2011). Dissolved organic carbon cycling and transformation. In E. Wolanski, & D. S. McLusky (Eds.), *Treatise on estuarine and coastal science* (Vol. 5, pp. 7–67). Waltham, MA: Academic Press.
- Bauer, J. E., Cai, W.-J., Raymond, P. A., Bianchi, T. S., Hopkinson, C. S., & Regnier, P. A. G. (2013). The changing carbon cycle of the coastal ocean. *Nature*, 504(7478), 61–70. <https://doi.org/10.1038/nature12857>
- Bauer, J. E., Druffel, E. R. M., Wolgast, D. M., & Griffin, S. (2001). Sources and cycling of dissolved and particulate organic radiocarbon in the northwest Atlantic continental margin. *Global Biogeochemical Cycles*, 15(3), 615–636. <https://doi.org/10.1029/2000GB001314>
- Bauer, J. E., Druffel, E. R. M., Wolgast, D. M., & Griffin, S. (2002). Temporal and regional variability in sources and cycling of DOC and POC in the northwest Atlantic continental shelf and slope. *Deep Sea Research Part II: Topical Studies in Oceanography*, 49(20), 4387–4419. [https://doi.org/10.1016/S0967-0645\(02\)00123-6](https://doi.org/10.1016/S0967-0645(02)00123-6)
- Beale, M. H., Hagan, M. T., & Demuth, H. B. (2018). Neural network toolbox. Retrieved from Natick, Massachusetts:
- Bjorrisen, P. K. (1988). Phytoplankton exudation of organic matter: Do healthy cells do it? *Limnology and Oceanography*, 33(1), 151–154. <https://doi.org/10.4319/lo.1988.33.1.0151>
- Blough, N. V., & Del Vecchio, R. (2002). Chapter 10—Chromophoric DOM in the coastal environment A2—Hansell, Dennis A. In C. A. Carlson (Ed.), *Biogeochemistry of Marine Dissolved Organic Matter*, (pp. 509–546). San Diego: Academic Press.
- Boicourt, W. C. (1992). Influences of circulation processes on dissolved oxygen in the Chesapeake Bay. In L. M. Smith, & M. G. D. E. (Eds.), *Oxygen dynamics in the Chesapeake Bay: a synthesis of recent research*, (pp. 7–59). College Park, Maryland: Maryland Sea Grant Publication.
- Boyle, E., Collier, R., Dengler, A. T., Edmond, J. M., Ng, A. C., & Stallard, R. F. (1974). On the chemical mass-balance in estuaries. *Geochimica et Cosmochimica Acta*, 38(11), 1719–1728. [https://doi.org/10.1016/0016-7037\(74\)90188-4](https://doi.org/10.1016/0016-7037(74)90188-4)
- Brewer, P. (2018). Coastal ocean warming adds to CO₂ burden. *Eos*, 99. <https://doi.org/10.1029/2018EO099877>
- Brezonik, P. L., Olmanson, L. G., Finlay, J. C., & Bauer, M. E. (2015). Factors affecting the measurement of CDOM by remote sensing of optically complex inland waters. *Remote Sensing of Environment*, 157, 199–215. <https://doi.org/10.1016/j.rse.2014.04.033>
- Burdige, D. J., & Homstead, J. (1994). Fluxes of dissolved organic carbon from Chesapeake Bay sediments. *Geochimica et Cosmochimica Acta*, 58(16), 3407–3424. [https://doi.org/10.1016/0016-7037\(94\)90095-7](https://doi.org/10.1016/0016-7037(94)90095-7)
- Cai, W. J., & Wang, Y. (1998). The chemistry, fluxes, and sources of carbon dioxide in the estuarine waters of the Satilla and Altamaha Rivers, Georgia. *Limnology and Oceanography*, 43(4), 657–668. <https://doi.org/10.4319/lo.1998.43.4.0657>
- Cai, W. J., Wiebe, W. J., Wang, Y., & Sheldon, J. E. (2000). Intertidal marsh as a source of dissolved inorganic carbon and a sink of nitrate in the Satilla River—Estuarine complex in the southeastern US. *Limnology and Oceanography*, 45(8), 1743–1752. <https://doi.org/10.4319/lo.2000.45.8.1743>

- Cao, F., Tzortziou, M., Hu, C., Mannino, A., Fichot, C. G., Del Vecchio, R., et al. (2018). Remote sensing retrievals of colored dissolved organic matter and dissolved organic carbon dynamics in North American estuaries and their margins. *Remote Sensing of Environment*, 205, 151–165. <https://doi.org/10.1016/j.rse.2017.11.014>
- Castro, M. S., Driscoll, C. T., Jordan, T. E., Reay, W. G., Boynton, W. R., Seitzinger, S. P., et al. (2001). Contribution of Atmospheric Deposition to the Total Nitrogen Loads to Thirty-Four Estuaries on the Atlantic and Gulf Coasts of the United States. In R. A. Valigura, et al. (Eds.), *Nitrogen Loading in Coastal Water Bodies: An Atmospheric Perspective* (pp. 77–106). <https://doi.org/10.1029/CE057p0077>
- Cerco, C. F., & Cole, T. (1993). Three-dimensional eutrophication model of Chesapeake Bay. *Journal of Environmental Engineering*, 119(6), 1006–1025. [https://doi.org/10.1061/\(ASCE\)0733-9372\(1993\)119:6\(1006\)](https://doi.org/10.1061/(ASCE)0733-9372(1993)119:6(1006))
- Ciais, P., Sabine, C., Bala, G., Bopp, L., Brovkin, V., Canadell, J., & Thornton, P. (2013). Carbon and other biogeochemical cycles. In T. F. Stocker, et al. (Eds.), *Climate change 2013: The Physical Science Basis. Contribution of Working Group I to the Fifth Assessment Report of the Intergovernmental Panel on Climate Change* (Chap. 6, pp. 465–570). Cambridge, United Kingdom and New York, NY, USA: Cambridge University Press.
- Crosswell, J. R., Anderson, I. C., Stanhope, J. W., Van Dam, B., Brush, M. J., Ensign, S., et al. (2017). Carbon budget of a shallow, lagoonal estuary: Transformations and source-sink dynamics along the river-estuary-ocean continuum. *Limnology and Oceanography*, 62(S1), S29–S45. <https://doi.org/10.1002/lno.10631>
- Cui, Q., He, X., Liu, Q., Bai, Y., Chen, C.-T. A., Chen, X., & Pan, D. (2018). Estimation of lateral DOC transport in marginal sea based on remote sensing and numerical simulation. *Journal of Geophysical Research: Oceans*, 123, 5525–5542. <https://doi.org/10.1029/2018JC014079>
- Da, F., Friedrichs, M. A. M., & St-Laurent, P. (2018). Impacts of atmospheric nitrogen deposition and coastal nitrogen fluxes on oxygen concentrations in Chesapeake Bay. *Journal of Geophysical Research: Oceans*, 123, 5004–5025. <https://doi.org/10.1029/2018JC014009>
- Decho, A. W., & Gutierrez, T. (2017). Microbial extracellular polymeric substances (EPSs) in ocean systems. *Frontiers in Microbiology*, 9, 1–21. <https://doi.org/10.3389/fmicb.2017.00922>
- Del Castillo, C. E., & Miller, R. L. (2008). On the use of ocean color remote sensing to measure the transport of dissolved organic carbon by the Mississippi River Plume. *Remote Sensing of Environment*, 112(3), 836–844. <https://doi.org/10.1016/j.rse.2007.06.015>
- Del Vecchio, R., & Blough, N. V. (2004). Spatial and seasonal distribution of chromophoric dissolved organic matter and dissolved organic carbon in the Middle Atlantic Bight. *Marine Chemistry*, 89(1–4), 169–187. <https://doi.org/10.1016/j.marchem.2004.02.027>
- Druon, J.-N., Mannino, A., Signorini, S. R., McClain, C. R., Friedrichs, M. A. M., Wilkin, J., & Fennel, K. (2010). Modeling the dynamics and export of dissolved organic matter in the Northeastern US continental shelf. *Estuarine, Coastal and Shelf Science*, 88(4), 488–507. <https://doi.org/10.1016/j.ecss.2010.05.010>
- Du, J., & Shen, J. (2016). Water residence time in Chesapeake Bay for 1980–2012. *Journal of Marine Systems*, 164, 101–111. <https://doi.org/10.1016/j.jmarsys.2016.08.011>
- Fairall, C. W., Bradley, E. F., Hare, J. E., Grachev, A. A., & Edson, J. B. (2003). Bulk parameterization of air–sea fluxes: Updates and verification for the COARE algorithm. *Journal of Climate*, 16, 571–591. [https://doi.org/10.1175/1520-0442\(2003\)016<0571:BPOASF>2.0.CO;2](https://doi.org/10.1175/1520-0442(2003)016<0571:BPOASF>2.0.CO;2)
- Feng, Y., Friedrichs, M. A. M., Wilkin, J., Tian, H., Yang, Q., Hofmann, E. E., & Hood, R. R. (2015). Chesapeake Bay nitrogen fluxes derived from a land-estuarine ocean biogeochemical modeling system: Model description, evaluation, and nitrogen budgets. *Journal of Geophysical Research: Biogeosciences*, 120, 1666–1695. <https://doi.org/10.1002/2015JG002931>
- Fichot, C. G., & Benner, R. (2011). A novel method to estimate DOC concentrations from CDOM absorption coefficients in coastal waters. *Geophysical Research Letters*, 38, L03610. <https://doi.org/10.1029/2010GL046152>
- Fichot, C. G., Lohrenz, S. E., & Benner, R. (2014). Pulsed, cross-shelf export of terrigenous dissolved organic carbon to the Gulf of Mexico. *Journal of Geophysical Research: Oceans*, 119, 1176–1194. <https://doi.org/10.1002/2013JC009424>
- Fisher, T. R., Hagy, J. III, & Rochelle-Newall, E. J. (1998). Dissolved and particulate organic carbon in Chesapeake Bay. *Estuaries*, 21(2), 215–229. <https://doi.org/10.2307/1352470>
- Ford, P., Tillman, P., Robson, B., & Webster, I. T. (2005). Organic carbon deliveries and their flow related dynamics in the Fitzroy estuary. *Marine Pollution Bulletin*, 51(1), 119–127. <https://doi.org/10.1016/j.marpolbul.2004.10.019>
- Fransner, F., Nycander, J., Mörth, C.-M., Humborg, C., Markus Meier, H. E., Hordoir, R., et al. (2016). Tracing terrestrial DOC in the Baltic Sea—A 3-D model study. *Global Biogeochemical Cycles*, 30, 134–148. <https://doi.org/10.1002/2014GB005078>
- Gazeau, F., Borges, A. V., Carlos, M., Iversen, N., Middelburg, J. J., Delille, B., & Gattuso, J.-P. (2005). Net ecosystem metabolism in a microtidal estuary (Randers Fjord, Denmark) evaluation of methods. *Marine Ecology Progress Series*, 301, 23–41. <https://doi.org/10.3354/meps301023>
- Guo, L., Santschi, P. H., & Warnken, K. W. (1995). Dynamics of dissolved organic carbon (DOC) in oceanic environments. *Limnology and Oceanography*, 40(8), 1392–1403. <https://doi.org/10.4319/lo.1995.40.8.1392>
- Harding, L. W., Mallonee, M. E., & Perry, E. S. (2002). Toward a predictive understanding of primary productivity in a temperate, partially stratified estuary. *Estuarine, Coastal and Shelf Science*, 55(3), 437–463. <https://doi.org/10.1006/ecss.2001.0917>
- Harvey, H. R., & Mannino, A. (2001). The chemical composition and cycling of particulate and macromolecular dissolved organic matter in temperate estuaries as revealed by molecular organic tracers. *Organic Geochemistry*, 32(4), 527–542. [https://doi.org/10.1016/S0146-6380\(00\)00193-5](https://doi.org/10.1016/S0146-6380(00)00193-5)
- Helms, J. R., Stubbins, A., Ritchie, J. D., Minor, E. C., Kieber, D. J., & Mopper, K. (2008). Absorption spectral slopes and slope ratios as indicators of molecular weight, source, and photobleaching of chromophoric dissolved organic matter. *Limnology and Oceanography*, 53(3), 955–969. <https://doi.org/10.4319/lo.2008.53.3.0955>
- Herrmann, M., Najjar, R. G., Kemp, W. M., Alexander, R. B., Boyer, E. W., Cai, W. J., et al. (2015). Net ecosystem production and organic carbon balance of U.S. East Coast estuaries: A synthesis approach. *Global Biogeochemical Cycles*, 29, 96–111. <https://doi.org/10.1002/2013GB004736>
- Hofmann, A. F., Soetaert, K., & Middelburg, J. J. (2008). Present nitrogen and carbon dynamics in the Scheldt estuary using a novel 1-D model. *Biogeochemistry*, 84(4), 981–1006. <https://doi.org/10.1017/bg-5-981-2008>
- Hoge, F. E., Williams, M. E., Swift, R. N., Yungel, J. K., & Vodacek, A. (1995). Satellite retrieval of the absorption coefficient of chromophoric dissolved organic matter in continental margins. *Journal of Geophysical Research*, 100(C12), 24,847–24,854. <https://doi.org/10.1029/95JC02561>
- Irby, I. D., & Friedrichs, M. A. M. (2019). Evaluating confidence in the impact of regulatory nutrient reduction on Chesapeake Bay water quality. *Estuaries and Coasts*, 42, 16–32. <https://doi.org/10.1007/s12237-018-0440-5>
- Jordan, T. E., & Correll, D. L. (1991). Continuous automated sampling of tidal exchanges of nutrients by brackish marshes. *Estuarine, Coastal and Shelf Science*, 32(6), 527–545. [https://doi.org/10.1016/0272-7714\(91\)90073-K](https://doi.org/10.1016/0272-7714(91)90073-K)

- Jordan, T. E., Correll, D. L., & Whigham, D. F. (1983). Nutrient flux in the Rhode River: tidal exchange of nutrients by brackish marshes. *Estuarine, Coastal and Shelf Science*, 17(6), 651–667. [https://doi.org/10.1016/0272-7714\(83\)90032-X](https://doi.org/10.1016/0272-7714(83)90032-X)
- Kaul, L. W., & Froelich, P. N. (1984). Modeling estuarine nutrient geochemistry in a simple system. *Geochimica et Cosmochimica Acta*, 48(7), 1417–1433. [https://doi.org/10.1016/0016-7037\(84\)90399-5](https://doi.org/10.1016/0016-7037(84)90399-5)
- Kemp, W. M., Boynton, W. R., Adolf, J. E., Boesch, D. F., Boicourt, W. C., Brush, G., et al. (2005). Eutrophication of Chesapeake Bay: Historical trends and ecological interactions. *Marine Ecology Progress Series*, 303, 1–29. <https://doi.org/10.3354/meps303001>
- Kemp, W. M., Smith, E. M., Marvin-DiPasquale, M., & Boynton, W. R. (1997). Organic carbon balance and net ecosystem metabolism in Chesapeake Bay. *Marine Ecology Progress Series*, 150(1/3), 229–248. <https://doi.org/10.3354/meps150229>
- Laruelle, G. G., Goossens, N., Arndt, S., Cai, W. J., & Regnier, P. (2017). Air–water CO₂ evasion from US East Coast estuaries. *Biogeosciences*, 14(9), 2441–2468. <https://doi.org/10.5194/bg-14-2441-2017>
- Lerczak, J. A., Geyer, W. R., & Chant, R. J. (2006). Mechanisms driving the time-dependent salt flux in a partially stratified estuary. *Journal of Physical Oceanography*, 36(12), 2296–2311. <https://doi.org/10.1175/jpo2959.1>
- Liss, P. S. (1976). Conservative and non-conservative behaviour of dissolved constituents during estuarine mixing. In J. D. Burton & P. S. Liss (Eds.), *Estuarine chemistry* (pp. 93–130). New York and London: Academic Press.
- Liu, M., Tian, H., Lu, C., Xu, X., Chen, G., & Ren, W. (2012). Effects of multiple environment stresses on evapotranspiration and runoff over eastern China. *Journal of Hydrology*, 426–427, 39–54. <https://doi.org/10.1016/j.jhydrol.2012.01.009>
- Luettich, R. A., & Westerink, J. J. (1991). A solution for the vertical variation of stress, rather than velocity, in a three-dimensional circulation model. *International Journal for Numerical Methods in Fluids*, 12(10), 911–928. <https://doi.org/10.1002/flid.1650121002>
- Maher, D. T., & Eyre, B. D. (2012). Carbon budgets for three autotrophic Australian estuaries: Implications for global estimates of the coastal air–water CO₂ flux. *Global Biogeochemical Cycles*, 26, GB1032. <https://doi.org/10.1029/2011GB004075>
- Mannino, A., & Harvey, H. R. (1999). Lipid composition in particulate and dissolved organic matter in the Delaware Estuary: Sources and diagenetic patterns. *Geochimica et Cosmochimica Acta*, 63(15), 2219–2235. [https://doi.org/10.1016/S0016-7037\(99\)00128-3](https://doi.org/10.1016/S0016-7037(99)00128-3)
- Mannino, A., & Harvey, H. R. (2000a). Biochemical composition of particles and dissolved organic matter along an estuarine gradient: Sources and implications for DOM reactivity. *Limnology and Oceanography*, 45(4), 775–788. <https://doi.org/10.4319/lo.2000.45.4.0775>
- Mannino, A., & Harvey, H. R. (2000b). Terrigenous dissolved organic matter along an estuarine gradient and its flux to the coastal ocean. *Organic Geochemistry*, 31(12), 1611–1625. [https://doi.org/10.1016/S0146-6380\(00\)00099-1](https://doi.org/10.1016/S0146-6380(00)00099-1)
- Mannino, A., Novak, M. G., Hooker, S. B., Hyde, K., & Aurin, D. (2014). Algorithm development and validation of CDOM properties for estuarine and continental shelf waters along the northeastern U.S. coast. *Remote Sensing of Environment*, 152, 576–602. <https://doi.org/10.1016/j.rse.2014.06.027>
- Mannino, A., Russ, M. E., & Hooker, S. B. (2008). Algorithm development and validation for satellite-derived distributions of DOC and CDOM in the US Middle Atlantic Bight. *Journal of Geophysical Research*, 113, C07051. <https://doi.org/10.1029/2007JC004493>
- Mannino, A., Signorini, S. R., Novak, M. G., Wilkin, J., Friedrichs, M. A. M., & Najjar, R. G. (2016). Dissolved organic carbon fluxes in the Middle Atlantic Bight: An integrated approach based on satellite data and ocean model products. *Journal of Geophysical Research: Biogeosciences*, 121, 312–336. <https://doi.org/10.1002/2015JG003031>
- Matsuoka, A., Boss, E., Babin, M., Karp-Boss, L., Hafez, M., Chekalyuk, A., & Bricaud, A. (2017). Pan-Arctic optical characteristics of colored dissolved organic matter: Tracing dissolved organic carbon in changing Arctic waters using satellite ocean color data. *Remote Sensing of Environment*, 200, 89–101. <https://doi.org/10.1016/j.rse.2017.08.009>
- McGuirk Flynn, A. (2008). Organic matter and nutrient cycling in a coastal plain estuary: Carbon, nitrogen, and phosphorus distributions, budgets, and fluxes. *Journal of Coastal Research*, 55, 76–94. <https://doi.org/10.2112/S155-010.1>
- Meng, F., Dai, M., Cao, Z., Wu, K., Zhao, X., Li, X., & Gan, J. (2017). Seasonal dynamics of dissolved organic carbon under complex circulation schemes on a large continental shelf: The northern South China Sea. *Journal of Geophysical Research: Oceans*, 122, 9415–9428. <https://doi.org/10.1002/2017JC013325>
- Mesinger, F., DiMego, G., Kalnay, E., Mitchell, K., Shafran, P. C., Ebisuzaki, W., et al. (2006). North American regional reanalysis: A long-term, consistent, high-resolution climate dataset for the North American domain, as a major improvement upon the earlier global reanalysis datasets in both resolution and accuracy. *Bulletin of the American Meteorological Society*, 87(3), 343–360. <https://doi.org/10.1175/BAMS-87-3-343>
- Mitra, S., Bianchi, T. S., Guo, L., & Santschi, P. H. (2000). Terrestrially derived dissolved organic matter in the Chesapeake Bay and the Middle Atlantic Bight. *Geochimica et Cosmochimica Acta*, 64(20), 3547–3557. [https://doi.org/10.1016/S0016-7037\(00\)00450-6](https://doi.org/10.1016/S0016-7037(00)00450-6)
- Mukai, A. Y., Westerink, J. J., Luettich, R. A., & Mark, D. (2002). *Eastcoast 2001, a tidal constituent database for the western North Atlantic, Gulf of Mexico, and Caribbean Sea (ERDC/CHL TR-02-24)*. Washington, D. C.: U.S. Army Corps of Engineers.
- Najjar, R., Patterson, L., & Graham, S. (2009). Climate simulations of major estuarine watersheds in the Mid-Atlantic region of the US. *Climatic Change*, 95(1), 139–168. <https://doi.org/10.1007/s10584-008-9521-y>
- Najjar, R. G., Herrmann, M., Alexander, R., Boyer, E. W., Burdige, D. J., Butman, D., et al. (2018). Carbon budget of tidal wetlands, estuaries, and shelf waters of Eastern North America. *Global Biogeochemical Cycles*, 32, 389–416. <https://doi.org/10.1002/2017GB005790>
- Nixon, S. W., Ammerman, J. W., Atkinson, L. P., Berounsky, V. M., Billen, G., Boicourt, W. C., et al. (1996). The fate of nitrogen and phosphorus at the land–sea margin of the North Atlantic Ocean. *Biogeochemistry*, 35(1), 141–180. <https://doi.org/10.1007/bf02179826>
- Officer, C. B. (1979). Discussion of the behaviour of nonconservative dissolved constituents in estuaries. *Estuarine and Coastal Marine Science*, 9(1), 91–94. [https://doi.org/10.1016/0302-3524\(79\)90009-4](https://doi.org/10.1016/0302-3524(79)90009-4)
- Peixoto, J. P., & Oort, A. H. (1992). *Physics of climate* (Vol. American Institute of Physics). New York, NY: American Institute of Physics.
- Pennock, J. R., & Sharp, J. H. (1986). Phytoplankton production in the Delaware estuary: temporal and spatial variability. *Marine Ecology Progress Series*, 34(1/2), 143–155. <https://doi.org/10.3354/meps034143>
- Pritchard, D. W. (1956). The dynamic structure of a coastal plain estuary. *Journal of Marine Research*, 15, 33–42.
- Pritchard, D. W. (1967). Observations of circulation in coastal plain estuaries. In G. H. Lauff (Ed.), *Estuaries*, (pp. 37–44). Washington, DC: American Association for the Advancement of Science.
- Raymond, P. A., & Bauer, J. E. (2001). DOC cycling in a temperate estuary: A mass balance approach using natural ¹⁴C and ¹³C isotopes. *Limnology and Oceanography*, 46(3), 655–667. <https://doi.org/10.4319/lo.2001.46.3.0655>
- Raymond, P. A., Bauer, J. E., & Cole, J. J. (2000). Atmospheric CO₂ evasion, dissolved inorganic carbon production, and net heterotrophy in the York River estuary. *Limnology and Oceanography*, 45(8), 1707–1717. <https://doi.org/10.4319/lo.2000.45.8.1707>
- Reimer, J. J., Wang, H., Vargas, R., & Cai, W.-J. (2017). Multidecadal fCO₂ increase along the United States southeast coastal margin. *Journal of Geophysical Research: Oceans*, 122, 10,061–10,072. <https://doi.org/10.1002/2017JC013170>
- Rochelle-Newall, E., & Fisher, T. (2002). Chromophoric dissolved organic matter and dissolved organic carbon in Chesapeake Bay. *Marine Chemistry*, 77(1), 23–41. [https://doi.org/10.1016/S0304-4203\(01\)00073-1](https://doi.org/10.1016/S0304-4203(01)00073-1)

- Roman, C. T., & Dalber, F. C. (1989). Organic carbon flux through a Delaware Bay salt marsh: tidal exchange, particle size distribution, and storms. *Marine Ecology Progress Series*, 54, 149–156. <https://doi.org/10.3354/meps054149>
- Ross, A. C., Najjar, R. G., Li, M., Lee, S. B., Zhang, F., & Wei, L. (2017). Fingerprints of sea level rise on changing tides in the Chesapeake and Delaware Bays. *Journal of Geophysical Research: Oceans*, 122, 8102–8125. <https://doi.org/10.1002/2017JC012887>
- Samanta, S., Dalai, T. K., Pattanaik, J. K., Rai, S. K., & Mazumdar, A. (2015). Dissolved inorganic carbon (DIC) and its $\delta^{13}\text{C}$ in the Ganga (Hooghly) River estuary, India: Evidence of DIC generation via organic carbon degradation and carbonate dissolution. *Geochimica et Cosmochimica Acta*, 165, 226–248. <https://doi.org/10.1016/j.gca.2015.05.040>
- Schubel, J. R., & Pritchard, D. W. (1986). Responses of upper Chesapeake Bay to variations in discharge of the Susquehanna River. *Estuaries*, 9(4), 236–249. <https://doi.org/10.2307/1352096>
- Sharp, J. H. (1977). Excretion of organic matter by marine phytoplankton: Do healthy cells do it? *Limnology and Oceanography*, 22, 381–399. <https://doi.org/10.4319/lo.1977.22.3.0381>
- Sharp, J. H., Cifuentes, L. A., Coffin, R. B., Pennock, J. R., & Wong, K.-C. (1986). The influence of river variability on the circulation, chemistry, and microbiology of the Delaware estuary. *Estuaries*, 9(4), 261–269. <https://doi.org/10.2307/1352098>
- Sharp, J. H., Yoshiyama, K., Parker, A. E., Schwartz, M. C., Curless, S. E., Beauregard, A. Y., et al. (2009). A biogeochemical view of estuarine eutrophication: Seasonal and spatial trends and correlations in the Delaware estuary. *Estuaries and Coasts*, 32(6), 1023–1043. <https://doi.org/10.1007/s12237-009-9210-8>
- Signorini, S. R., Mannino, A., Najjar, R. G., Friedrichs, M. A. M., Cai, W.-J., Salisbury, J., et al. (2013). Surface ocean $p\text{CO}_2$ seasonality and sea-air CO_2 flux estimates for the North American east coast. *Journal of Geophysical Research: Oceans*, 118, 5439–5460. <https://doi.org/10.1002/jgrc.20369>
- Slonecker, E. T., Jones, D. K., & Pellerin, B. A. (2016). The new Landsat 8 potential for remote sensing of colored dissolved organic matter (CDOM). *Marine Pollution Bulletin*, 107(2), 518–527. <https://doi.org/10.1016/j.marpolbul.2016.02.076>
- Smullen, J. T., Sharp, J. H., Garvine, R. W., & Haskin, H. H. (1983). River flow and salinity. In J. Sharp (Ed.), *The Delaware estuary: Research as background for estuarine management and development. Report to Delaware River and Bay Authority* (pp. 9–25). Newark, Delaware: University of Delaware (College of Marine Studies) and New Jersey Marine Sciences Consortium.
- Soetaert, K., & Herman, P. M. J. (1995). Carbon flows in the Westerschelde estuary (The Netherlands) evaluated by means of an ecosystem model (MOSES). *Hydrobiologia*, 311(1), 247–266. <https://doi.org/10.1007/bf00008584>
- Son, Y. B., Gardner, W. D., Mishonov, A. V., & Richardson, M. J. (2009). Multispectral remote-sensing algorithms for particulate organic carbon (POC): The Gulf of Mexico. *Remote Sensing of Environment*, 113(1), 50–61. <https://doi.org/10.1016/j.rse.2008.08.011>
- Stanley, D. (2001). An annotated summary of nitrogen loading to US estuaries. In R. A. Valigura, et al. (Eds.), *Nitrogen loading in coastal water bodies: An atmospheric perspective* (pp. 227–252). Washington, DC: American Geophysical Union.
- Tabatabai, S. A. (2017). *Physical and biogeochemical modeling in Delaware estuary*. (Doctor of Philosophy. New Brunswick, NJ: Rutgers, The State University of New Jersey.
- Tian, H., Lu, C., Chen, G., Xu, X., & Liu, M. (2011). Climate and land use controls over terrestrial water use efficiency in monsoon Asia. *Ecohydrology*, 4(2), 322–340. <https://doi.org/10.1002/eco.2016>
- Tian, H., Yang, Q., Najjar, R. G., Ren, W., Friedrichs, M. A. M., Hopkinson, C. S., & Pan, S. (2015). Anthropogenic and climatic influences on carbon fluxes from eastern North America to the Atlantic Ocean: A process-based modeling study. *Journal of Geophysical Research: Biogeosciences*, 120, 757–772. <https://doi.org/10.1002/2014JG002760>
- Valle-Levinson, A., Li, C., Royer, T. C., & Atkinson, L. P. (1998). Flow patterns at the Chesapeake Bay entrance. *Continental Shelf Research*, 18(10), 1157–1177. [https://doi.org/10.1016/S0278-4343\(98\)00036-3](https://doi.org/10.1016/S0278-4343(98)00036-3)
- Vanderborcht, J.-P., Folmer, I. M., Aguilera, D. R., Uhrenholdt, T., & Regnier, P. (2007). Reactive-transport modelling of C, N, and O_2 in a river–estuarine–coastal zone system: Application to the Scheldt estuary. *Marine Chemistry*, 106(1), 92–110. <https://doi.org/10.1016/j.marchem.2006.06.006>
- Volta, C., Laruelle, G. G., & Regnier, P. (2016). Regional carbon and CO_2 budgets of North Sea tidal estuaries. *Estuarine, Coastal and Shelf Science*, 176, 76–90. <https://doi.org/10.1016/j.ecss.2016.04.007>
- Walsh, J., D. Wuebbles, L. Authors, K. Hayhoe, K. Kunkel, N. Cli-matic, et al., (2013). Our changingclimate. <http://ncadac.globalchange.gov/download/NCAJan11-2013-publicreviewdraft-chap2-climate.pdf>, accessed May 2013.
- Wang, Z. A., & Cai, W.-J. (2004). Carbon dioxide degassing and inorganic carbon export from a marsh-dominated estuary (the Duplin River): A marsh CO_2 pump. *Limnology and Oceanography*, 49(2), 341–354. <https://doi.org/10.4319/lo.2004.49.2.0341>
- Winter, P. E. D., Schlacherl, T. A., & Baird, D. (1996). Carbon flux between an estuary and the ocean: A case for outwelling. *Hydrobiologia*, 337(1), 123–132. <https://doi.org/10.1007/bf00028513>
- Wu, K., Dai, M., Li, X., Meng, F., Chen, J., & Lin, J. (2017). Dynamics and production of dissolved organic carbon in a large continental shelf system under the influence of both river plume and coastal upwelling. *Limnology and Oceanography*, 62(3), 973–988. <https://doi.org/10.1002/lno.10479>
- Yang, Q., Tian, H., Friedrichs, M. A. M., Hopkinson, C. S., Lu, C., & Najjar, R. G. (2015). Increased nitrogen export from eastern North America to the Atlantic Ocean due to climatic and anthropogenic changes during 1901–2008. *Journal of Geophysical Research: Biogeosciences*, 120, 1046–1068. <https://doi.org/10.1002/2014JG002763>
- Yang, Q., Tian, H., Friedrichs, M. A. M., Liu, M., Li, X., & Yang, J. (2015). Hydrological responses to climate and land-use changes along the North American East Coast: A 110-year historical reconstruction. *JAWRA Journal of the American Water Resources Association*, 51(1), 47–67. <https://doi.org/10.1111/jawr.12232>